2009-12-22

Verification of the "Energy Accumulation in Waves Travelling through a Checkerboard Dielectric Material Structure in Space-time" Using Spice Simulations

Gajanan Balkrishna Samant
Worcester Polytechnic Institute

Verification of the

"Energy Accumulation in Waves Travelling through a Checkerboard Dielectric Material Structure in Space-time"

Using Spice Simulations

By

Gajanan B. Samant

A Thesis Dissertation
Submitted to the Faculty of

Worcester Polytechnic Institute

In partial fulfillment of the requirements for the
Degree of Master of Science
In
Electrical and Computer Engineering

December 2009

Approved By:

Professor Konstantin Lurie, Thesis Advisor

Professor Reinhold Ludwig, Thesis Advisor

Professor Suzanne Weekes, Committee Member

ABSTRACT

Recently, there has been some good interest in the field of Dynamic Materials, also referred to as Spatio-Temporal Composites. These materials have been theoretically attributed to show ability to switch their electromagnetic properties in time, as contrast to the spatial variations shown by regular materials of non-dynamic nature, existing naturally. Though there is no exhibition of dynamic material in nature yet, there are suggestions for its synthesis. This paper follows the idea of using standard lossless transmission line model approximating a material substance. Such a material though not truly homogeneous, could be made to vary its properties in time. The aim of this work is to test this idea for its functional efficiency in comparison to analytical results obtained from earlier works on the subject. We make use of Spice simulation for this.

An important aspect of this work is to facilitate the dynamic operations in a static environment. Almost all the simulators available today like Spice, ADS, etc intrinsically provide no ability for parameter variations in time. Nonetheless, we make use of certain popular tricks to implement circuits imitating the dynamic circuit components we need. Such implementations are separately tested to demonstrate their success in providing us with the dynamic environment we desire. Finally, within the limitations of the computing capabilities, we could successfully show an agreement between the results obtained and the existing theory.

Acknowledgement

I take this opportunity to show my sincere appreciation for all the support and guidance offered to me by every individual involved in this thesis, either directly or indirectly.

First and foremost my heartfelt thanks to Prof. Konstantin Lurie who had been a backbone for this work. He has been a master guide to find the solution to most obstacles I faced in the process of completion of this work. His excitement and persistent efforts motivated me to work harder, and achieve the results. I express my gratitude towards him for all his contribution in this work which includes editing my manuscripts.

I would like to thank Prof. Reinhold Ludwig for his support in every possible way. He offered himself as an advisor for this work, and provided a moral support by being there whenever I needed him with any kind of help, may it be some academic counseling, or paperwork formalities, or even personal recommendations. He has been a motivating factor towards completion of this thesis.

I thank Prof. Alexander Emanuel for his short but valuable guidance. He made himself available in spite of his other academic commitments keeping him busy. His has been an extremely valuable contribution by suggesting the ideas which ultimately came to rescue me from a point of halt.

I thank Prof. John McNeill for offering his help in chalking out initial plan of approach for practical development of the ideas in this paper. His ideas form the base for immediate future work in the subject matter.

I thank Prof. Weekes, who showed her readiness to provide help as and when needed. I admire her kindness in offering herself as a committee, and willingness to help me in all ways needed. Her suggestion and comments on the manuscript were very useful and uplifted the quality of work.

I wish to thank Mr. Siamak Najafi, who worked very quickly to provide me access to the computers in his labs, and giving me special permissions to save data on them which was very necessary for my work. I also thank my friend Nandish Desai who came up with this suggestion of approaching Mr. Najafi for help with faster computations.

My thank goes to all the active members of the yahoo group on LTspice, who were constantly active to assist with my queries regarding LTspice. They also provided some very useful material which helped me learn Spice.

Finally, I thank my parents and Lord Almighty for making me a person worth handling this work.

Table of Content

List of Figures

List of symbols

E: Electric field vector
B**:** Magnetic flux density
H: Magnetic field vector
D: Charge density
ϵ: Dielectric permittivity
μ: Magnetic permeability
∇: Del operator
γ: Wave impedance
a: Phase velocity of wave scaled to checkerboard units
t: Time axis
w: Wave energy density
τ: Temporal period
n: Structural parameter for checkerboard associated with temporal period
δ: Spatial period
m: Structural parameter for checkerboard associated with spatial period
z: Space axis
u: A field potential defining time integral of electric field
v: A field potential defining space integral of magnetic flux density
R: Riemann invariant for right moving wave
L: Riemann invariant for left moving wave
A: Wave amplitude
λ: Wavelength
f: A function defining the average speed of waves in checkerboard
V: Voltage
Φ: Magnetic flux associated with an inductor
L: inductance
Q: charge across a capacitor
C: Capacitance
I: Current
Δ: Delta
$\frac{d}{dt}$: Time derivative operator
$\int dt$: Time integral operator
B: 'Arbitrary behavior current/voltage source' in LTspice
V: voltage source in LTspice
l: Number of LC units in the checkerboard
v: Phase velocity of waves in MKS units

k: number of temporal switchings in the checkerboard

List of tables

1. Energy Accumulation in Waves Travelling through a Checkerboard Dielectric Material Structure in Space-time

1.1. Introduction

With advancement in the material technology seen in the recent years, there has been some good attention in the field of Metamaterials. Metamaterials are artificially engineered materials exhibiting properties which may not be readily available in nature. These materials usually gain their properties from structure rather than composition, using the inclusion of small inhomogeneities to enact effective macroscopic behavior [1]. Even though the term metamaterials have been predominantly used to suggest the materials with negative refractive indices, the actual term encompass variety of synthetic materials including dynamic materials.

Dynamic materials as the name suggests posses the ability to switch their material properties in time. Even though the concept is so very apparent in our day to day lives, there is no natural material exhibiting such a property. As with all metamaterials, the characteristic of this material comes by arrangements at smaller structured blocks comprising the material. There have been certain suggestions for methods to implement dynamic materials. One such method is to model the material using a standard lossless transmission line model with variable circuit elements [2]. We, in this paper, make use of this idea to imitate a dynamic material varying its electromagnetic properties in time, and study its interaction with electromagnetic waves. Dynamic materials when thus arranged in space gives a 2D structure on space-time planes, hence often referred to as spatio-temporal composites. Already some good amount of theoretical work has been done in the subject by Prof. K. A. Lurie and Prof. S. L. Weekes [3][4][5][6][7][8][9][10][11]. The numerical analysis predicts a certain behavioral pattern for interaction of EM waves with such composite structures. There is a curiosity to verify these results with practical implementation of such spatio-temporal material composites. To this end, as a first step we test a transmission line approach by simulating it on a software environment, and get a better idea about the practical considerations before diving into physical construction.

This work aims to verify the analytical results of interaction between EM wave and spatio-temporal material composite by running simulations in Spice. LTspice is freely available and standard software for such electrical circuit simulations, but just like any other simulator in market, it falls short of providing the dynamic environment we desire for our application. We aim to construct a transmission line with elements which can vary their property value in time. But no simulator has intrinsic provisions to vary the parameter value in time. It allows us to define the values of such parameters before the beginning of the execution, and cannot be

varied once the execution begins. This was the first and the most intriguing challenge towards building a code which imitates the dynamic material structure. As a solution to this we have made use of existing tricks to model variable elements in Spice [12][13][14]. Such a technique mimics the behavior of standard static elements, and provides a convenient way to vary the properties as many times we desire during the same execution. Later in the paper, such techniques have been elaborated for inductor and capacitor modeling.

Beside the main goal of verification of the predictions from the numerical computations using electrical circuit simulations, this work also serves to set ideas for a real-world physical implementation of the spatio-temporal structure. It gives us a hint towards the practical constraints and problems we might face while developing a real world prototype of our structure. Even though the parameter values we have worked with are chosen to aid computer simulations, and may not be feasible for practical constructions, we did verify the principle and can be positive about the actual hardware construction.

Maxwell's equations written for a dielectric medium with variable properties have the form [15]

$$\nabla \times \boldsymbol{E} = -\boldsymbol{B}_t \,, \quad \nabla \cdot \boldsymbol{B} = 0 \,,$$

$$\nabla \times \boldsymbol{H} = -\boldsymbol{D}_t \,, \quad \nabla \cdot \boldsymbol{D} = 0 \,,$$

where $\boldsymbol{E}, \boldsymbol{H}$ are the electric and magnetic field vectors linked with $\boldsymbol{D}, \boldsymbol{B}$ through the material relations

$$\boldsymbol{D} = \epsilon \boldsymbol{E}, \qquad \boldsymbol{B} = \mu \boldsymbol{H},$$

in which $\epsilon = \epsilon(x, y, z, t)$, $\mu = \mu(x, y, z, t)$ are, respectively, the dielectric permittivity and the magnetic permeability of the immovable substance; these parameters can vary in both space and time.

In what follows, we consider plane electromagnetic waves propagating along the z-axis; for such a wave

$$\boldsymbol{E} = E\boldsymbol{j}, \quad \boldsymbol{B} = B\boldsymbol{i}, \quad \boldsymbol{D} = D\boldsymbol{j}, \quad \boldsymbol{H} = H\boldsymbol{i}, \tag{1}$$

and the Maxwell's equations take the form

$$E_z = B_t \,, \qquad H_z = D_t \,, \tag{2}$$

with

$$\boldsymbol{D} = \epsilon \boldsymbol{E} \,, \qquad \boldsymbol{B} = \mu \boldsymbol{H} \,. \tag{3}$$

We assume that the material properties μ, ϵ depend on z, t. Specifically, we will allow for two immovable material constituents: material 1 with properties μ_1, ϵ_1, and material 2 with properties μ_2, ϵ_2. Throughout the text, we will assume that the wave impedance

$$\gamma = \sqrt{\frac{\mu}{\epsilon}}$$

is the same for both materials: $\gamma_1 = \gamma_2$. The materials therefore differ only in the values of the phase velocity

$$a = \frac{1}{\sqrt{\mu\epsilon}},$$

so that $a_1 \neq a_2$. We will chose $a_2 > a_1$.

1.2 Spatial Interface: $z = z_0$

If materials $1(\mu_1, \epsilon_1)$ and $2(\mu_2, \epsilon_2)$ are separated by the interface $z = z_0$, then on such an interface the electric and magnetic fields are continuous:

$$E_1 = E_2, \qquad H_1 = H_2, \tag{4}$$

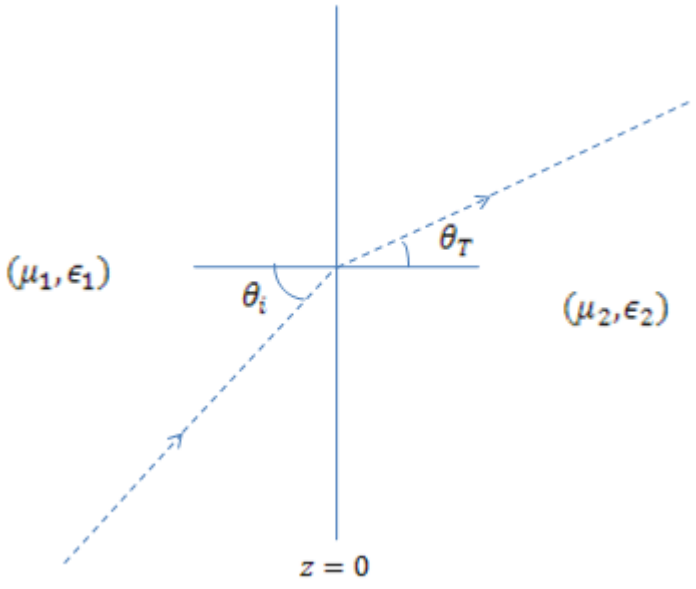

Figure 1. Wave propagation through a spatial interface

Once $\gamma_1 = \gamma_2$, there is no reflection on the spatial interface, so the incident wave gives birth to only one secondary wave which is a transmission wave travelling through adjacent material with different wavelength but the same frequency.

1.3 Temporal Interface: $t = t_0$

Consider a wave train entirely trapped in material 1 (may be infinitely extending in space), and travelling with a velocity determined by the material parameters μ_1,ϵ_1, and a frequency determined by the source. If such a medium is step-transformed ("switched") to another medium with parameters μ_2,ϵ_2, then it is interesting to study the wave behavior at the instant of switching, as shown.

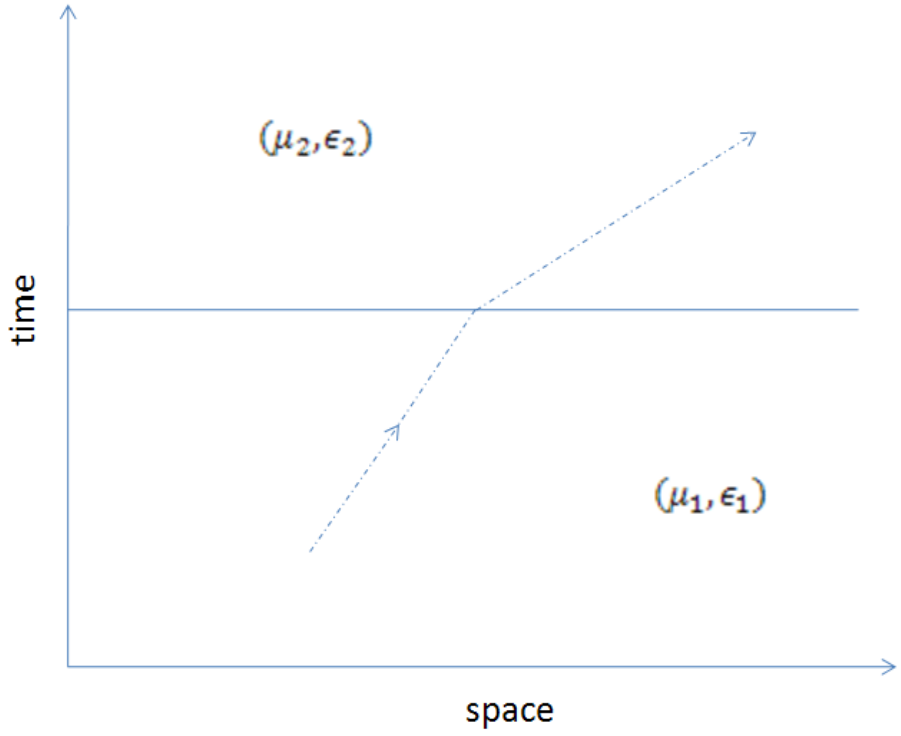

Figure 2. Wave propagation through a temporal interface

As before, only the phase velocity is affected as the medium parameters are changed in time. This phenomenon is very different than the spatial transfer of wave from one medium to another. The EM wave in the material responds to change in μ and ϵ, but since this change is

temporal, the compatibility conditions for the fields at time $t = t_0$ differ from $eq^n s$. (4) that hold on a spatial interface. At the temporal switching of the medium, we observe the continuity of D and B:

$$D_1 = D_2, \qquad B_1 = B_2. \tag{5}$$

Similarly to a spatial transition, a temporal switching gives birth to only one secondary wave if $\gamma_1 = \gamma_2$. This wave will be of different frequency but same wavelength, and will travel in material 2 once it emerges after the moment of switching [16][17].

1.4. Energy transformation at the Temporal Interface

A temporal switching in the medium properties induces changes in E and H; as a consequence, the wave energy density w is also changed [16][17]. The exact relation, proven later, says that

$$w_2 = (\frac{a_2}{a_1})w_1 ,$$

where a_1, w_1, a_2, w_2 are the velocities and energy densities of the waves in material 1 and material 2, respectively. This is the most impressive feature of temporal switching which can be used for practical applications. The apparent deviation from energy conservation law is resolved when we consider the work done by an external agent at the moment of switching, against the electromagnetic forces.

2. Temporal Laminate

Assume that we maintain successive alternation of two materials in time. The material assembly would then take the form of a ***temporal laminate,*** as shown here:

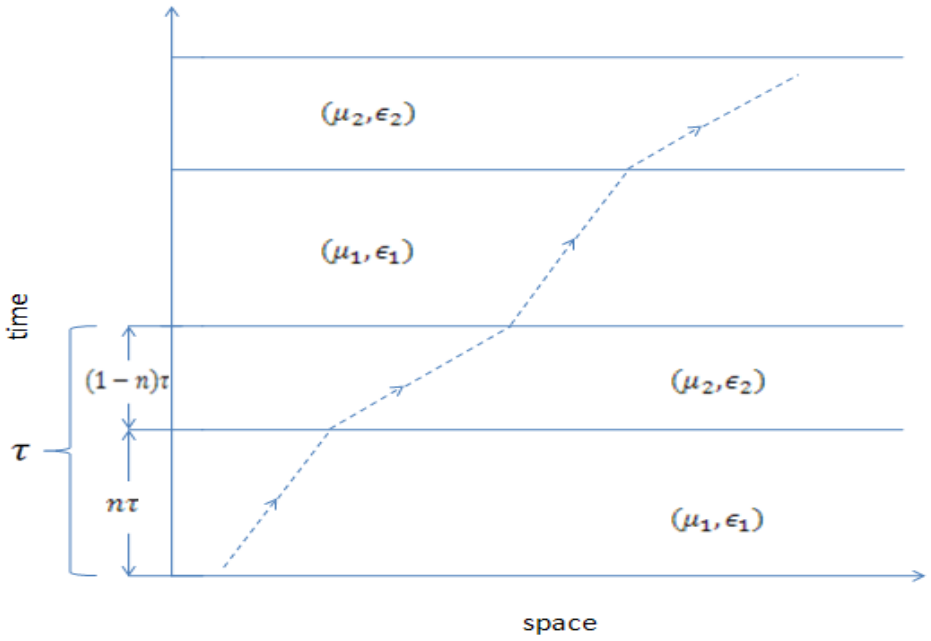

Figure 3. A temporal laminate structure

From the figure 3, we observe that the temporal material period is τ. Each material has its own share in the temporal period; material $1(\mu_1,\epsilon_1)$ is maintained from $t = 0 \ to \ t = n\tau$, while material $2(\mu_2,\epsilon_2)$ stays active from $t = n\tau \ to \ t = \tau$. It can be easily seen that, after one period, the net energy becomes

$$w_3 = (\frac{a_1}{a_2})w_2$$

$$= \left(\frac{a_1}{a_2}\right)\left(\frac{a_2}{a_1}\right)w_1$$

$$= w_1 \ .$$

So, there is no energy change over a period in a temporal laminate, hence the net energy change over any duration of time involving multiple periods is zero. This discourages us from employing a temporal laminate structure for practical use.

We want, however, to change this situation by offering a different (non- laminate) material structure in space-time - a structure capable of *managing the energy accumulation*. A temporal laminate has failed to secure such accumulation because the travelling wave loses its energy at

the moment when the wave enters material 1, with slower phase velocity. So to avoid this energy loss, the wave should find some other way into material 1, and that may become possible if the wave would enter material 1 across the ***spatial, not temporal*** interface. So, we arrive at the idea of testing a *rectangular* material structure in space-time; specifically, we try a checkerboard geometry.

3. Checkerboard

We aim for 'wise' arrangement of two materials in space, and for an appropriate switching of them from one to another, such that, ***"wave always enters material 1 from material 2 through a spatial interface (with no energy change), and it always enters material 2 from material 1 through a temporal interface (when it gains energy)".*** Such arrangement leads to a double periodic structure on a space-time plot, known as checkerboard pattern. This pattern would provide a net gain over one temporal period, which is also over a spatial period (double periodicity). As a result, contrary to the case of temporal laminates, we could harness the advantage of checkerboard for practical applications. ***The key problem is whether a checkerboard structure is capable of supporting the required characteristic pattern in space-time. We will see below that this question can be given a positive answer.***

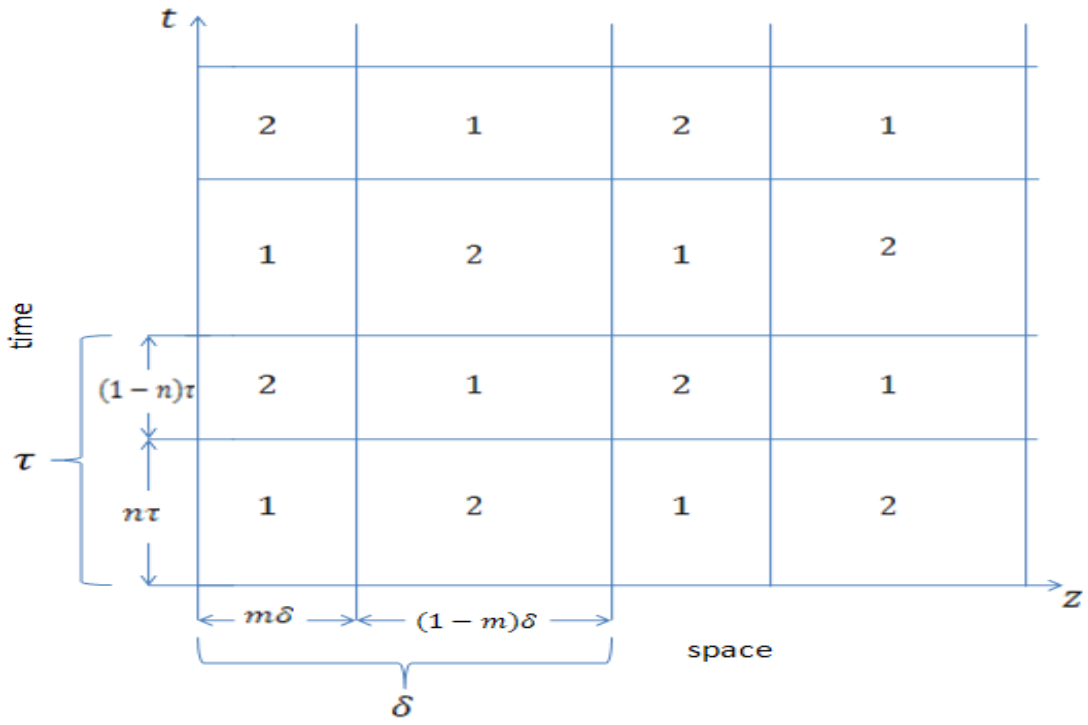

Figure 4. A checkerboard structure

The checkerboard structure is double periodic, with temporal period similar to that in a laminate, while in the spatial period δ, material 1 occupies a segment from $z = 0 \ \ to \ \ z = m\delta$, and material 2 - a segment from $z = m\delta \ \ to \ \ z = \ \delta$. As seen in the figure above, this double periodic structure repeats itself in space, as well as in time.

3.1. Mathematical Treatment of Wave Motion through the Checkerboard

$Eq^n s.(2)$ will be satisfied if we introduce potentials u and v through the relations

$$E = \ u_t \ , \qquad B = \ u_z \ , \qquad H = \ v_t \ , \qquad D = \ v_z \ . \tag{6}$$

$Eq^n s.(3)$ then reduce to the system

$$\epsilon u_t = \ v_z \ , \qquad u_z = \ \mu v_t \ . \tag{7}$$

We now eliminate ϵ and μ from $eq^n s.(7)$ by using the wave impedance γ and phase velocity a, defined as

$$\gamma = \sqrt{\frac{\mu}{\epsilon}} \ ,$$

$$a = \frac{1}{\sqrt{\mu\epsilon}} \ .$$

Hence, $eq^n s.(7)$ can be written as

$$u_t = \ \gamma a v_z, \qquad \gamma v_t = a u_z.$$

If $\gamma_1 = \ \gamma_2$, then this system is same as

$$R_t + \ aR_z = 0, \qquad L_t - \ aL_z = 0, \tag{8}$$

where

$$R = u - \ \gamma v, \qquad L = u + \ \gamma v,$$

are the Riemann invariants for the right moving wave, and the left moving wave, respectively. Since $\gamma_1 = \ \gamma_2$, in $eq^n s.(8)$ we apply a_1 for material 1, and a_2 for material 2. We will get back to $eq^n s.(8)$ later.

3.2. Wave Behavior at the Spatial Boundary

Consider an EM wave travelling in material 1(μ_1, ϵ_1) in a checkerboard. When the wave hits the spatial boundary separating this material from material 2(μ_2, ϵ_2), we generally observe a wave reflected back into the material 1, and another wave transmitted into material 2, as shown below:

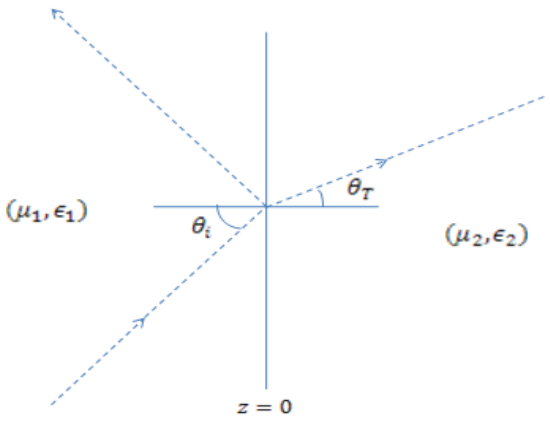

Figure 5. Refracted and reflected wave at the spatial boundary

From $eq^n s.(7)$ the wave u_1 in material 1 can be represented as –

$$u_1 = u_i + u_r$$
$$= A_I e^{\lambda(t - z/a_1)} + A_R e^{\lambda(t + z/a_1)},$$

where u_i and u_r are the incident and reflected waves, respectively. Note the sign of space variable z in the above solution. The transmitted wave can similarly be written as –

$$u_2 = u_T = A_T e^{\lambda(t - z/a_2)}.$$

To find the relation between the amplitudes of A_I, A_R and A_T, we use the conditions (4) on the interface $z = 0$. These conditions together with $eq^n s.(7), (8)$, yield

$$-\frac{1}{\gamma_1} u_i + \frac{1}{\gamma_1} u_r = -\frac{1}{\gamma_2} u_T \quad , \qquad \text{(i)}$$

$$u_i + u_r = u_T \quad . \qquad \text{(ii)}$$

By solving (i) and (ii), we get

$$u_r = \left(\frac{\gamma_1 - \gamma_2}{\gamma_1 + \gamma_2}\right) u_i \, , \qquad u_T = \left(\frac{2\gamma_2}{\gamma_1 + \gamma_2}\right) u_i \, .$$

Thus, the *reflected wave* is given by

$$u_r = \left(\frac{\gamma_1-\gamma_2}{\gamma_1+\gamma_2}\right) A_I e^{\lambda(t+z/a_1)} \quad , \qquad v_r = \frac{1}{\gamma_1}\left(\frac{\gamma_1-\gamma_2}{\gamma_1+\gamma_2}\right) A_I e^{\lambda(t+z/a_1)} \quad , \qquad (9a)$$

and the *transmitted wave* is given as

$$u_T = \left(\frac{2\gamma_2}{\gamma_1+\gamma_2}\right) A_I e^{\lambda(t+z/a_1)} \quad , \qquad v_T = -\frac{1}{\gamma_1}\left(\frac{2\gamma_2}{\gamma_1+\gamma_2}\right) A_I e^{\lambda(t+z/a_1)} \quad . \qquad (9b)$$

From, $eq^n.(9a)$ we can see there is no reflected wave if $\gamma_1 = \gamma_2$, which is the case for our checkerboard materials. We thus confirmed what has been said before about the absence of reflection.

3.3. Wave Behavior at the Temporal Boundary

We have already stated that, at the temporal boundary, there also will be only one secondary wave if the wave impedances of both materials match [16]. Now, it's time to show this mathematically.

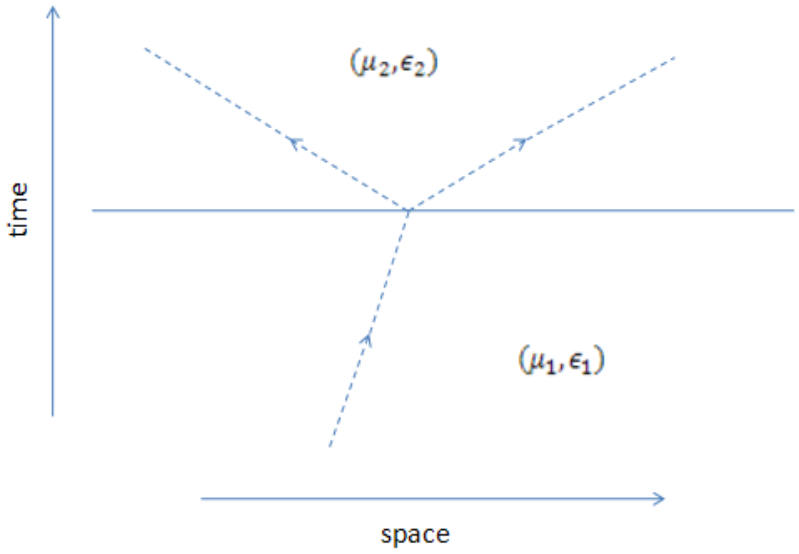

Figure 6. Forward moving and backward moving wave at the temporal boundary

The wave u_1 in material $1(\mu_1,\epsilon_1)$, is given by $eq^n s.(7)$ as

$$u_1 = u_i = A_I e^{\lambda_1(t-z/a_1)} \, ,$$

while the wave in material $2(\mu_2,\epsilon_2)$ can be represented as

$$u_2 = u_F + u_B$$
$$= A_F e^{\lambda_2 (t - z/a_2)} + A_B e^{\lambda_2 (t + z/a_2)} .$$

Here, u_i is the incident wave in material 1, while u_F and u_B are the forward-moving wave and backward-moving wave in material 2. Note, that by forward-moving and backward-moving, we mean spatial movement, since no wave can move back in time.

To find relation between the three waves, we use the boundary conditions (5). These $eq^n s$. together with (6) and (7), yield

$$\frac{1}{\gamma_1} u_i = \frac{1}{\gamma_2} u_B + \frac{1}{\gamma_2} u_F \ , \qquad \text{(iii)}$$

$$u_i + u_B = u_F \ . \qquad \text{(iv)}$$

By solving (iii) and (iv), we get

$$u_B = \left(\frac{\gamma_2 - \gamma_1}{2\gamma_1} \right) u_i \ ,$$

$$u_F = \left(\frac{\gamma_1 + \gamma_2}{2\gamma_1} \right) u_i \ .$$

Hence, the wave solution in material 2 is given as –

$$u_2 = u_F + u_B \ ,$$

$$u_2 = \frac{A_I}{2} \left\{ \left(\frac{\gamma_1 + \gamma_2}{\gamma_1} \right) e^{\lambda_2 (t - z/a_2)} + \left(\frac{\gamma_2 - \gamma_1}{\gamma_1} \right) e^{\lambda_2 (t + z/a_2)} \right\} \ , \qquad \text{(10a)}$$

$$v_2 = \frac{1}{\gamma_1} \frac{A_I}{2} \left\{ \left(\frac{\gamma_1 + \gamma_2}{\gamma_1} \right) e^{\lambda_2 (t - z/a_2)} - \left(\frac{\gamma_2 - \gamma_1}{\gamma_1} \right) e^{\lambda_2 (t + z/a_2)} \right\} \ . \qquad \text{(10b)}$$

But, for our application, the checkerboard materials have equal wave impedance, so $\gamma_1 = \gamma_2$, and from $eq^n s$. (10a) and (10b), we conclude that, similarly to the spatial case, there is no reflection from temporal interface, i.e. there is no backward-moving wave in the checkerboard.

We again state an important attribute of checkerboard, supported by both observations made so far: No reflection from spatial interfaces, and no backward-moving wave originating from temporal interfaces. As a result, any wave will travel along its own characteristic path without

any branching. And the waves for Riemann invariants introduced above (see $eq^n.(7)$) will travel totally independent of each other.

3.4. Previous Work

Now we are ready to answer the key question posted before, i.e., whether a checkerboard is capable of supporting the characteristic paths that secure the energy accumulation. As we will see in this section, the answer to this question is positive. It has been shown that, for certain ranges of material parameters m, n, a_1, a_2 of a checkerboard, the characteristic paths related to the Riemann invariant R, come into distinct groups that approach some selected characteristics playing the role of **limit cycles** [16][18]. The characteristics concentrate into dense arrays that enter material 1 across the spatial interface and leave it across the temporal interface, as desired to ensure the energy accumulation. An example of this situation is given in figure (7), below. Though this illustration is related to the travel of an R-wave, the effect will be word for word the same for an L-wave as well.

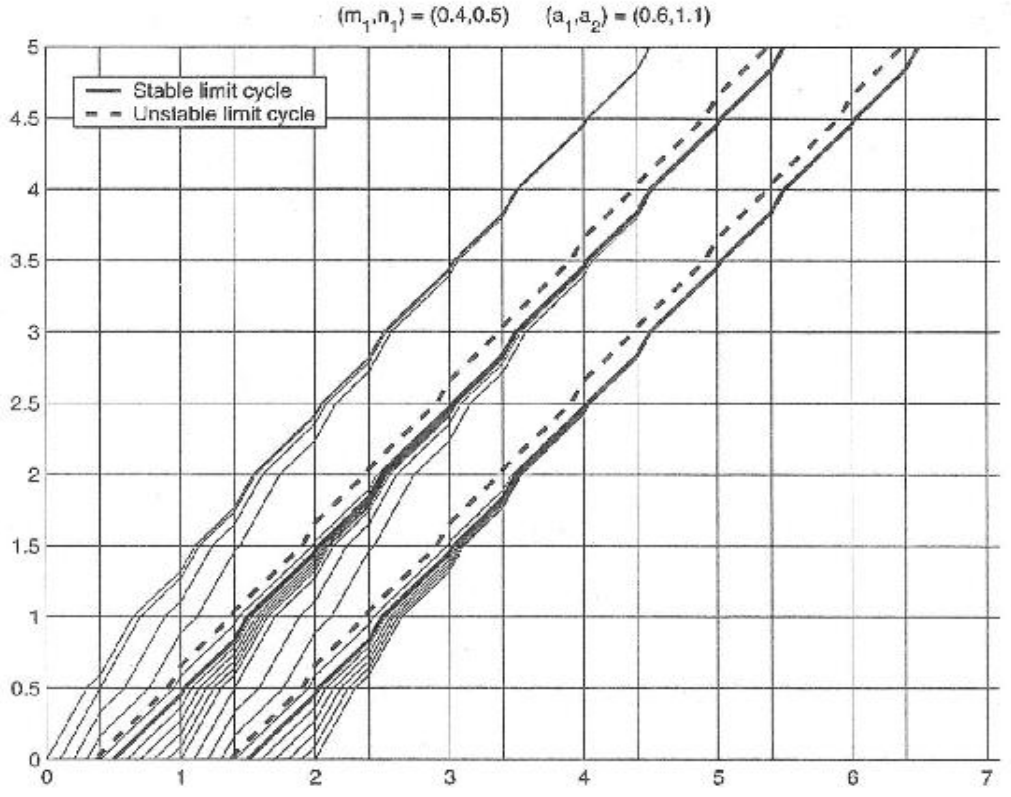

. 2. Limit cycles in the checkerboard structure with $a_{(1)} = 0.6$, $a_{(2)} = 1.1$, $m_1 = 0.4$, $n_1 = 0.5$.

Figure 7. Limit cycles in the checkerboard structure

We consider the structure with parameters $m_1 = 0.4, n_1 = 0.5, a_1 = 0.6, a_2 = 1.1$. The figure represents the paths of right-going R-disturbances which originate on the interval [0,2] at time 0. Time is measured along the vertical axis of this figure. The vertical and the horizontal lines define the checkerboard arrangement. It is clear to see that within each period, the group of paths in the figure (7) separate into two distinct arrays that each converges to its own limiting path ("limit cycle") after a few time periods. The limit paths (shown in bold) are called cycles because the trajectory pattern cycles of repeats. Such cycles are parallel to each other and have a common average slope equal to 1. Each cycle is stable; it attracts trajectories which originate on the initial manifold at the left and right of the point of origination of the cycle itself. In the example given, the cycles originate around $z = 0.5$ and $z = 1.5$ at time 0, and are indicated by the paths in bold. There is one limit cycle per spatial period. Successive stable limit cycles are separated by an unstable limit cycles (shown punctured). After close numerical inspection, we find that unstable limit cycle originate, at time 0, at points $n + 0.375$ for integers n, contrary to $n + 0.4953$ for stable limit cycles.

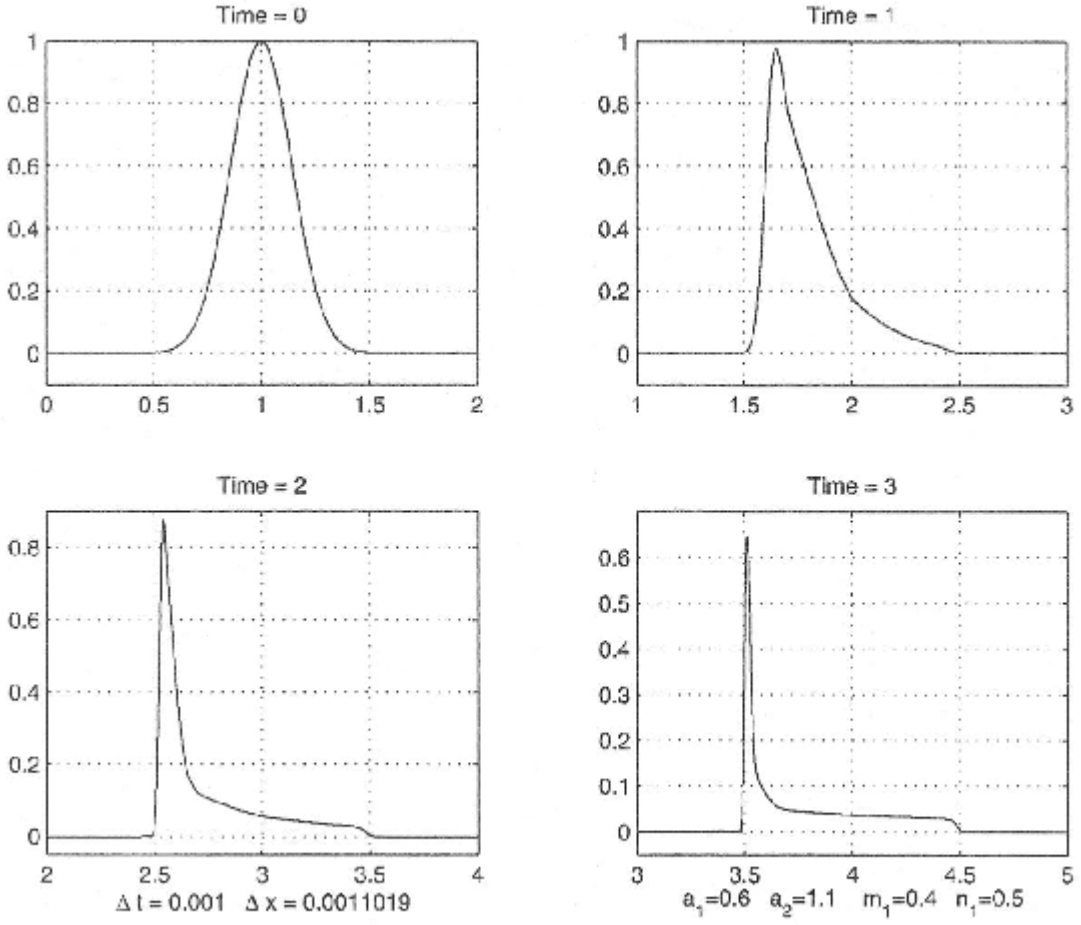

Evolution of a disturbance through a structure with $m_1 = 0.4$, $n_1 = 0.5$, $a_{(1)} = 0.6$ and $a_{(2)} = 1.1$.

Figure 8. Evolution of a disturbance through a structure

This convergence phenomenon manifests itself through concentration of the initial disturbance, and is illustrated in the solution profile sequence of above figure. The vertical axis is u, and z is on the horizontal axis. The profiles are computed from system (2) via a finite volume scheme. The initial disturbance is a Gaussian; we may regard it as having support on [0.5, 1.5]. We show evolution profiles up to time 3; the speed of the disturbance is seen to be 1. As the disturbance travels through the checkerboard material, the information that was initially spread over the region [0.5, 1.35] has, roughly speaking, by time 3, concentrated within the narrower region [3.5, 3.65]. The data is compressed as expected by trajectory behavior illustrated in the earlier figure. The information that was initially associated with z values in [1.35, 1.37] has, by time 3, been spread over the interval [3.65, 4.4] giving there almost constant state, while the rest of the solution changes more rapidly over [4.4, 4.5].

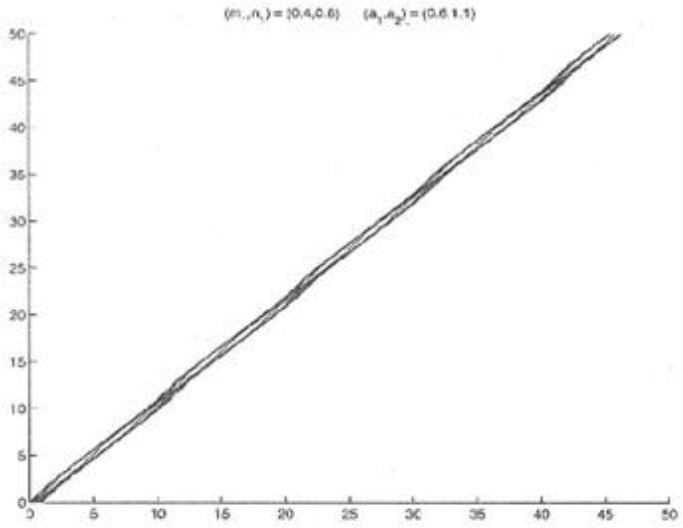

Low frequency pattern in trajectories through structure with $m_1 = 0.4, n_1 = 0.8, a_{(1)} = 0.6$ and $a_{(2)} = 1.1$.

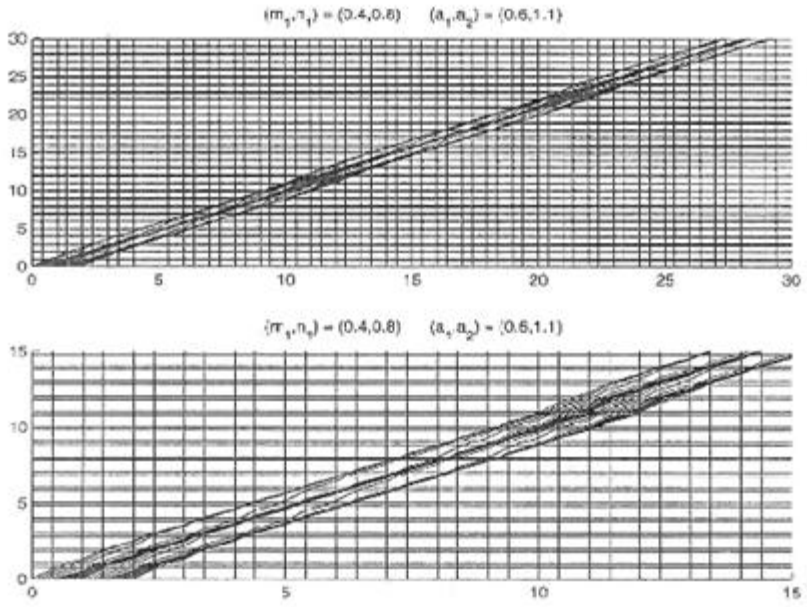

Closer view of wave trajectories through structure with $m_1 = 0.4$, $n_1 = 0.8$, $a_{(1)} = 0.6$ and $a_{(2)} = 1.1$.

Figure 9. Wave trajectories through checkerboard for n = 0.8

Next we consider the structure with the same values of a_i, m_i as before but with $n_1 = 0.8$. Unlike the first structure, the paths in figures above do not demonstrate stable convergence to isolated asymptotic routes. Instead, the trajectories engage in a regular pattern of drift towards and then away from the would-be limit cycles. This trend is periodic and the wavelength of this pattern is about 10 times the period of the structure itself. From the trajectories, we compute that the average speed of the disturbances is roughly 0.9.

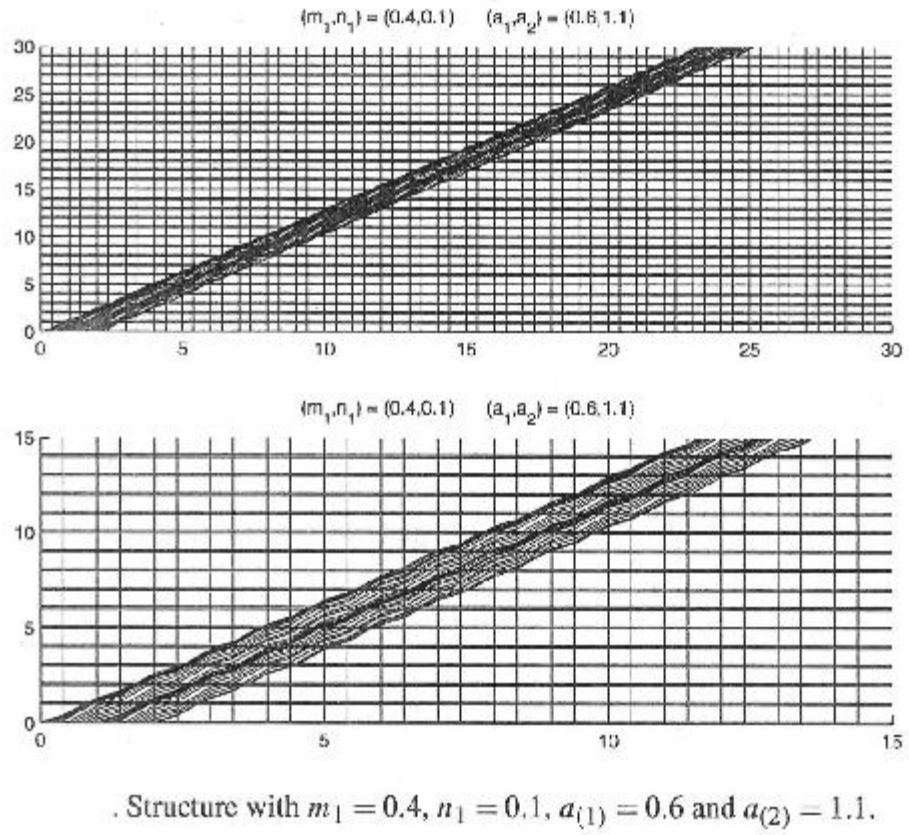

. Structure with $m_1 = 0.4$, $n_1 = 0.1$, $a_{(1)} = 0.6$ and $a_{(2)} - 1.1$.

Figure 10. Wave trajectories through the checkerboard for n = 0.1

If we then reduce n_1 to 0.1, then we see very little remnants of the existence of limit cycles. The wave trajectories more of less occupy the entire strip as seen in the above figure. The average asymptotic speed of these paths is roughly 0.77.

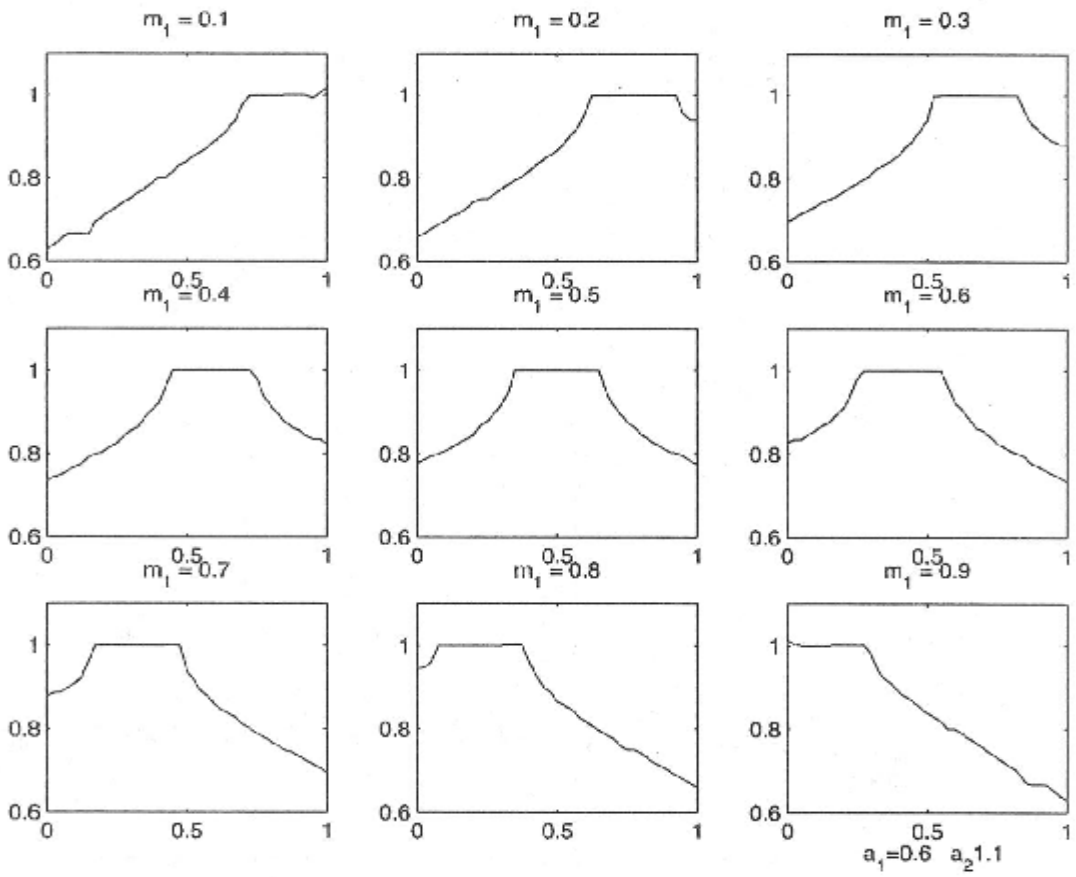

Wave speeds as a function of m_1 and n_1 for $a_{(1)} = 0.6$ and $a_{(2)} = 1.1$.

Figure 11. Graphical observation of plateau

The four parameters a_1, a_2, m_1, n_1 determine the checkerboard material, and hence determine the manner in which disturbances travel through such structures. In the three examples presented above, a_1, a_2 and m_1 were fixed, and by varying the value of n_1 only, we are able to see different trajectory behavior and different average speeds. In the above figure, we plot graphs of average speed versus n_1 for a sequence of m_1 values. Define the speed in the structures as $f(m_1, n_1)$. Notice that $f(m, n) = f(1 - m, 1 - n)$. This is so because, in space-time, each period of the structure with volume fraction (m, n) is made up of an $m \times n$ and an $(1 - m) \times (1 - n)$ rectangles of material 1 and the rest is filled with material 2. Thus, the checkerboard structure with volume fraction (m, n) is the same as that with volume fraction $(1 - m, 1 - n)$.

In several of the plots, we see intervals of n_1 for which $f(m_1, n_1)$ is constant for a given m_1 value; we call these "plateaux" and refer to the associated structure as "being on a plateau."

By inspecting the above plots, it is seen that for $a_1 = 0.6$ and $a_2 = 1.1$, there are always plateaux corresponding to a speed equal to unity. In the first example of this section where we observed the existence of stable limit cycles, we had $(m_1, n_1) = (0.4, 0.5)$. The propagation speed in such a structure is $1 = f(0.4, 0.5)$, and this material puts itself on the plateau of the fourth plot of the series shown above. The structure shown above, with $n_1 = 0.8$ and $n_1 = 0.1$ are not on a plateau and do not exhibit limit cycles.

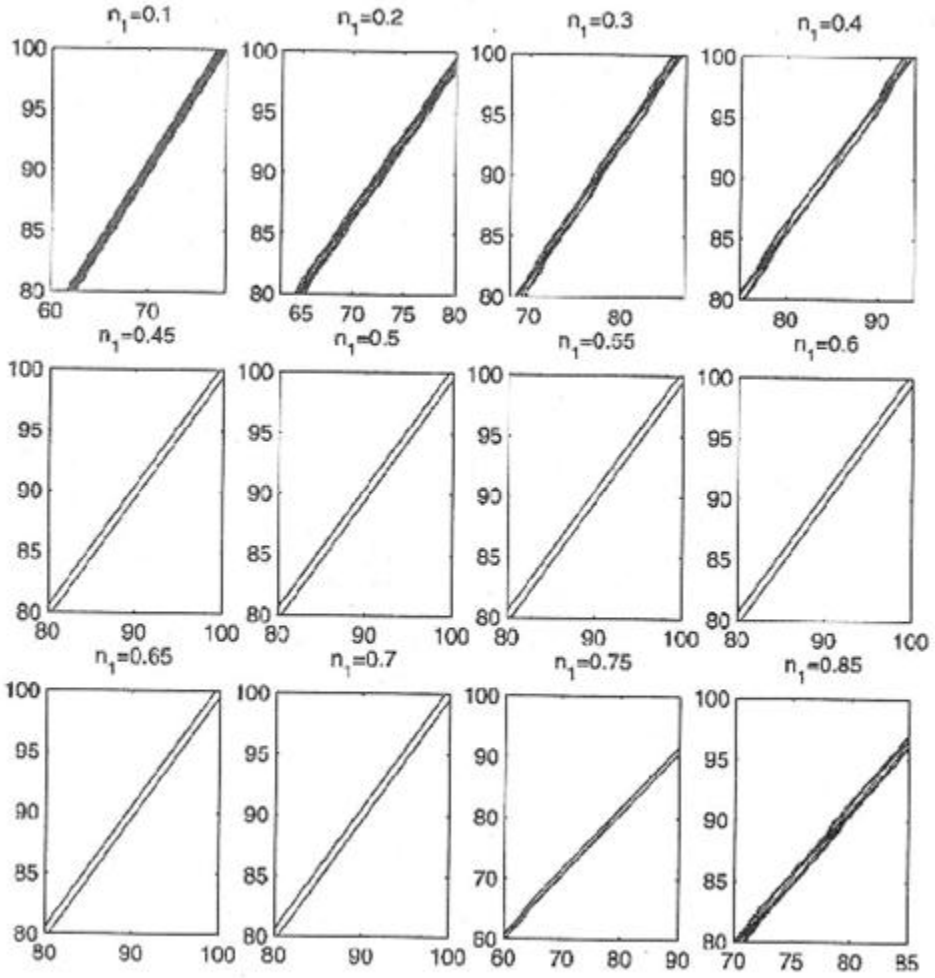

Trajectories in material with $a_{(1)} = 0.6$, $a_{(2)} = 1.1$, $m_1 = 0.4$ and n_1 as indicated.

Figure 12. Trajectories in material with varying parameter n

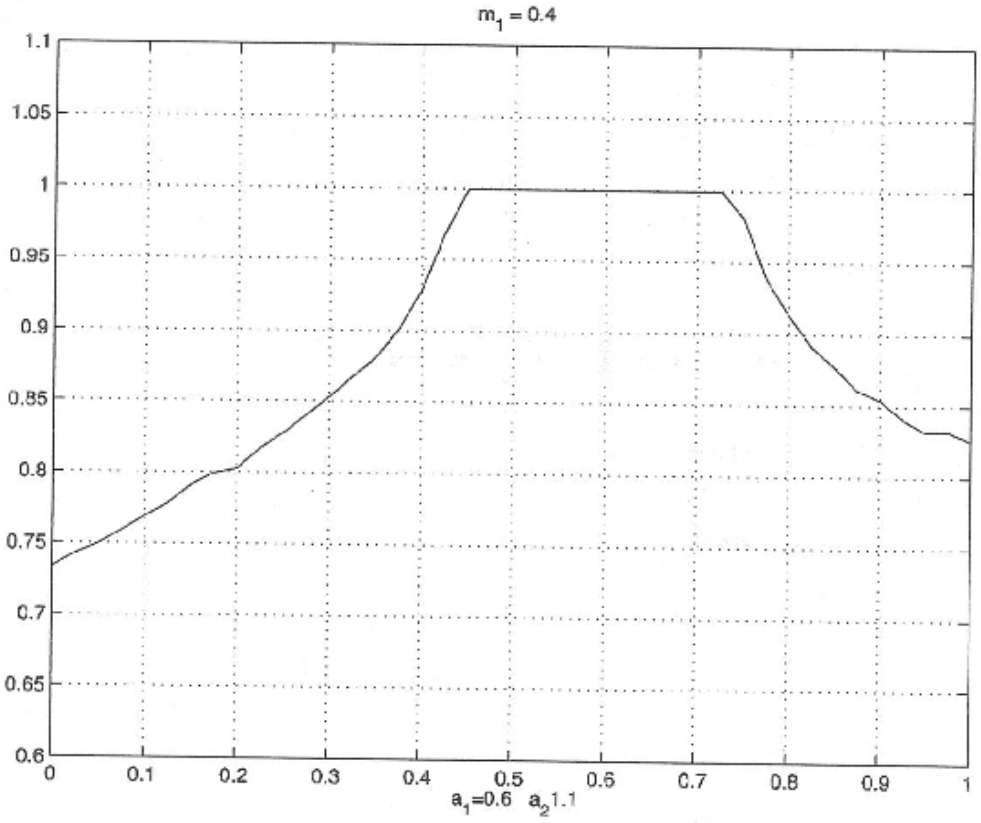

Figure 13. Graphical representation of a plateau

Figures above give portions of trajectories which originate on [0, 1] at time 0 in twelve checkerboard structures distinguished only by their values of n_1. The other parameter values are $a_1 = 0.6,\ a_2 = 1.1,\ m_1 = 0.4$. By comparing the values of n_1 which yield stable limit cycles with the location of the plateau in the velocity - n_1 graph for $m_1 = 0.4$ in the figure above, we propose the following hypothesis:

3.5. **Hypothesis:** *A structure is on a plateau if and only if the structure yields stable limit cycles.*

A structure yields two limit cycles, one stable and the other unstable, if and only if the structure is on plateau, i.e., the following two pairs of inequalities hold simultaneously [18]:

$$\frac{a_1\tau + \left(1 - \frac{a_1}{a_2}\right)m - \delta}{a_1 - a_2} \leq n \leq \frac{a_1\tau + \left(1 - \frac{a_2}{a_1}\right)m - \delta}{a_1 - a_2}$$

$$\frac{m - a_2\tau + \frac{a_2}{a_1}(\delta - m)}{a_1 - a_2} \leq n \leq \frac{m - a_2\tau + \frac{a_1}{a_2}(\delta - m)}{a_1 - a_2}$$

4. Schematic Circuit Formation:

In the above description, we studied propagation of a plane electromagnetic wave in one spatial dimension through a dielectric material structure that exhibits spatial-temporal property change. Now we are going to imitate such propagation by using a transmission line, with electrical parameters L and C, variable in space and time. The equations that govern the wave propagation along such a line are identical with equations (2) and (3), in which we have to change the symbols as follows

$$E \longrightarrow V, \qquad B \longrightarrow \Phi, \quad D \longrightarrow Q, \quad H \longrightarrow I, \qquad \epsilon \longrightarrow C, \qquad \mu \longrightarrow L.$$

In this list, V denotes the voltage, Φ denotes the magnetic flux associated with the inductance L , Q is the charge across the capacitor C, and I is the current.

We use the following model of a transmission line

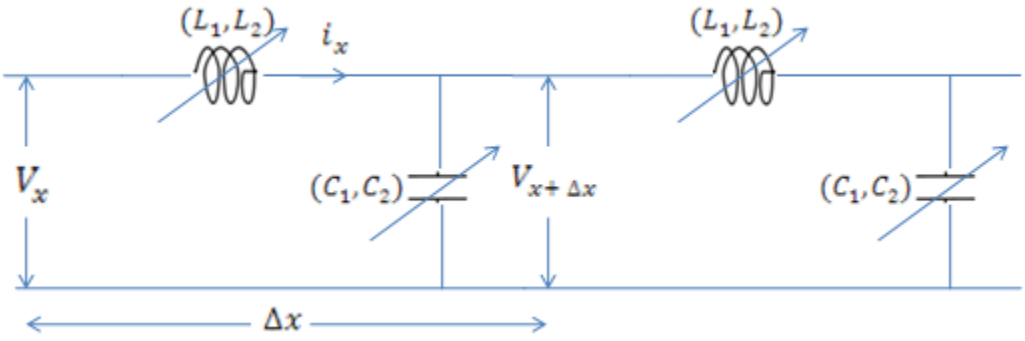

Figure 14. Standard lossless transmission line model with variable elements

Our application of checkerboard demands switching of the material parameter pairs (L, C) particularly in time. This change should go in accordance with the following

$$\begin{aligned} \gamma_1 = \gamma_2 \quad &\Longrightarrow \quad \frac{L_1}{C_1} = \frac{L_2}{C_2}, \\ a_1 < a_2 \quad &\Longrightarrow \quad L_1 C_1 > L_2 C_2 \,. \end{aligned} \tag{10}$$

4.1. Concept of Variable Inductors and Capacitors

When we talk about variable passive elements like inductors and capacitors, we have in our mind same behavioral characteristic of standard static elements. So basically we need something which is behaviorally exactly similar to its static counterpart, while being endowed with a special feature of abruptly changing its property value as and when signaled. As such, the output of a circuit involving these elements should be exactly same as that of the one involving a static element.

Consider a simple differentiator circuit, involving a capacitor as its integral part performing the differentiation function. Clearly the quality of the differentiator, and hence the output will be affected by any change in the value of C [19]. Below we show the standard RC differentiator circuits, with two different values of C and their corresponding outputs. The difference in the output waveforms (Blue) is clearly apparent.

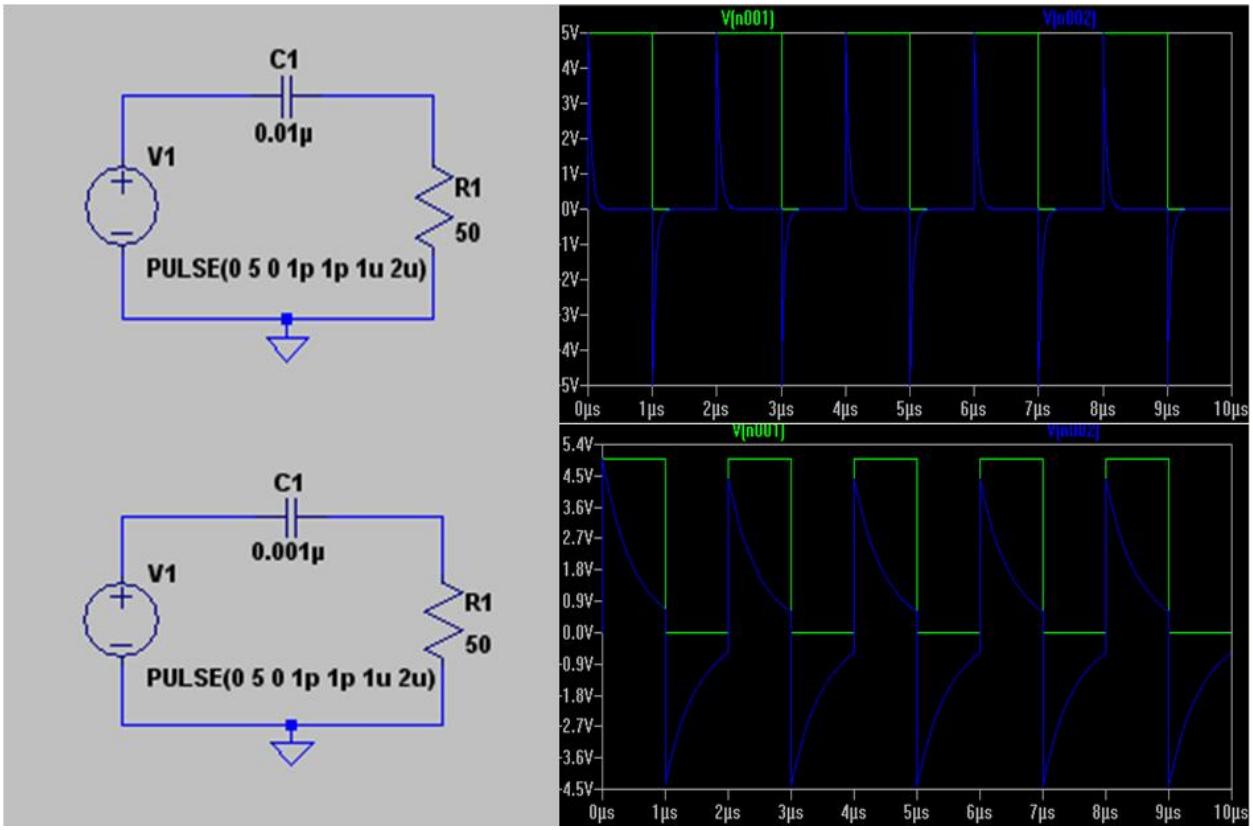

Figure 15. RC circuits and their outputs for different values of C

Looking at the plots above, we do get some idea of what the plots with variable capacitor must look like. Assuming the variable capacitor abruptly switches in value from $0.01\mu F$ to $0.001\ \mu F$

at time instant, say, $4\mu sec$, we expect the plot before and beyond this time instant to vary from each other in accordance with above plots. See the graph below

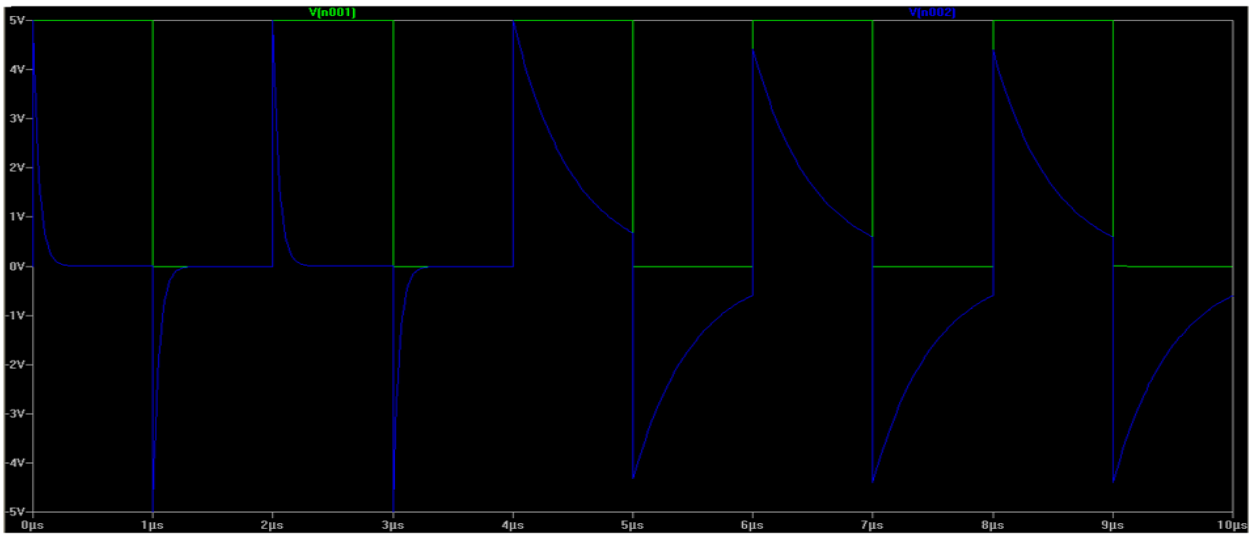

Figure 16. Output of an RC circuit with variable C switched at time $4\mu sec$

And that is exactly what we expect, given the constraint that the charge over the capacitor is preserved naturally when the C value undergoes a change. And this is precisely what would happen with real elements, since charge and flux preservation is a natural phenomenon upon which our application relies. The above plot was obtained from a Spice circuit which behaves like a 'true' static capacitor, but comes with an advantage of variability in its property value. We would discuss about the details of this scheme later, but for the time being we can have a look at differentiator circuit involving a variable capacitor.

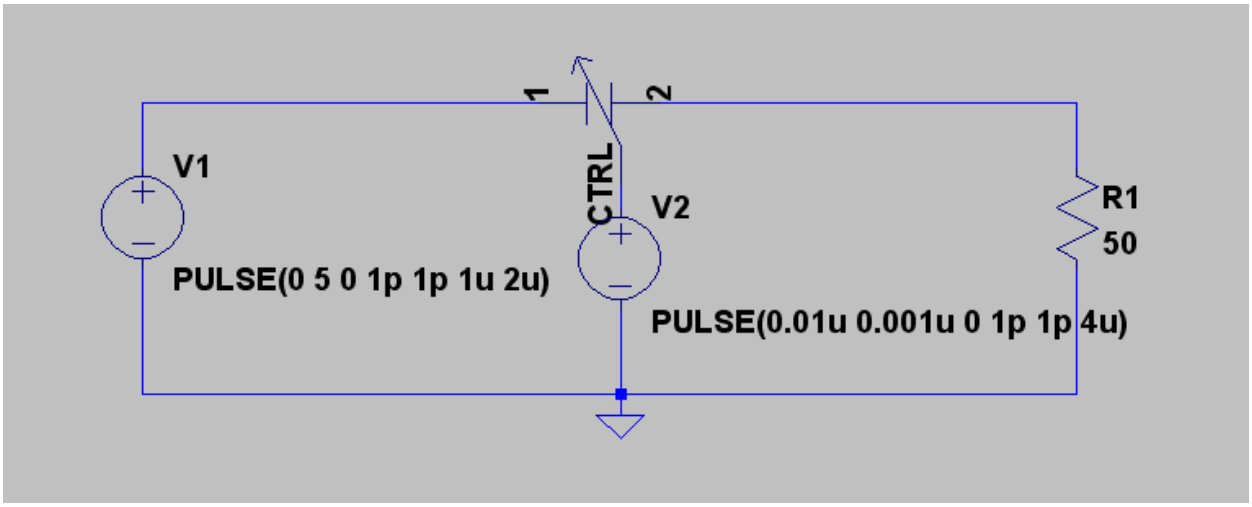

Figure 17. RC circuit with variable C

We can see that the variable capacitor circuit it similar to the static one, except the variable capacitor has an extra port CTRL for controlling the capacitance value. There is an additional voltage source V2 which generates a dc voltage of 0.01 μV until 4 μsec, while later rise to 0.001 μV at a rise time of 1 $psec$. Also note how the voltage of V2 assumes the capacitance value to be achieved. Why this is the case, will be understood when we establish the variable element schemes.

The above discussion also holds true in case of a variable inductor. In the figures below we will observe the varying outputs from circuits involving different value of L, and how variable inductor circuit achieves same results but with the same unique circuit [20].

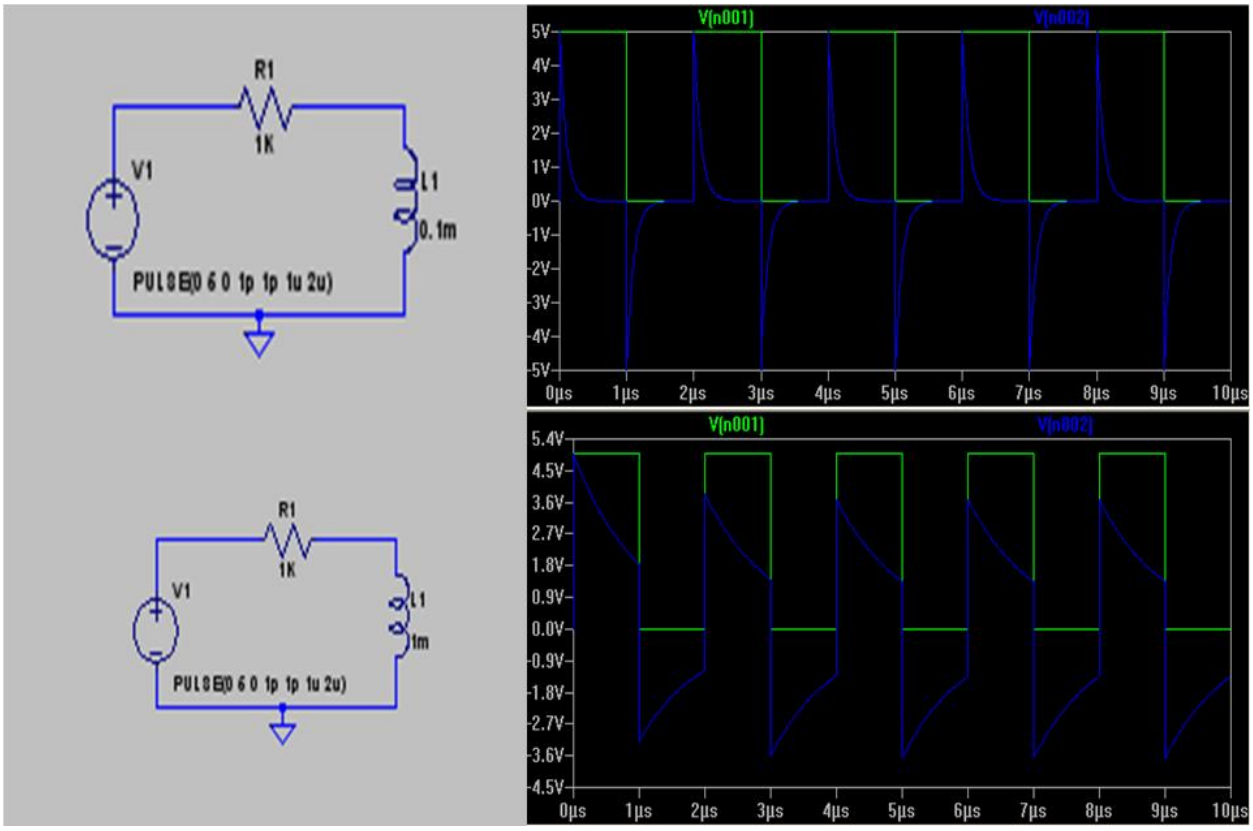

Figure 18. LR circuits with their outputs for different values of L

And with the variable inductor –

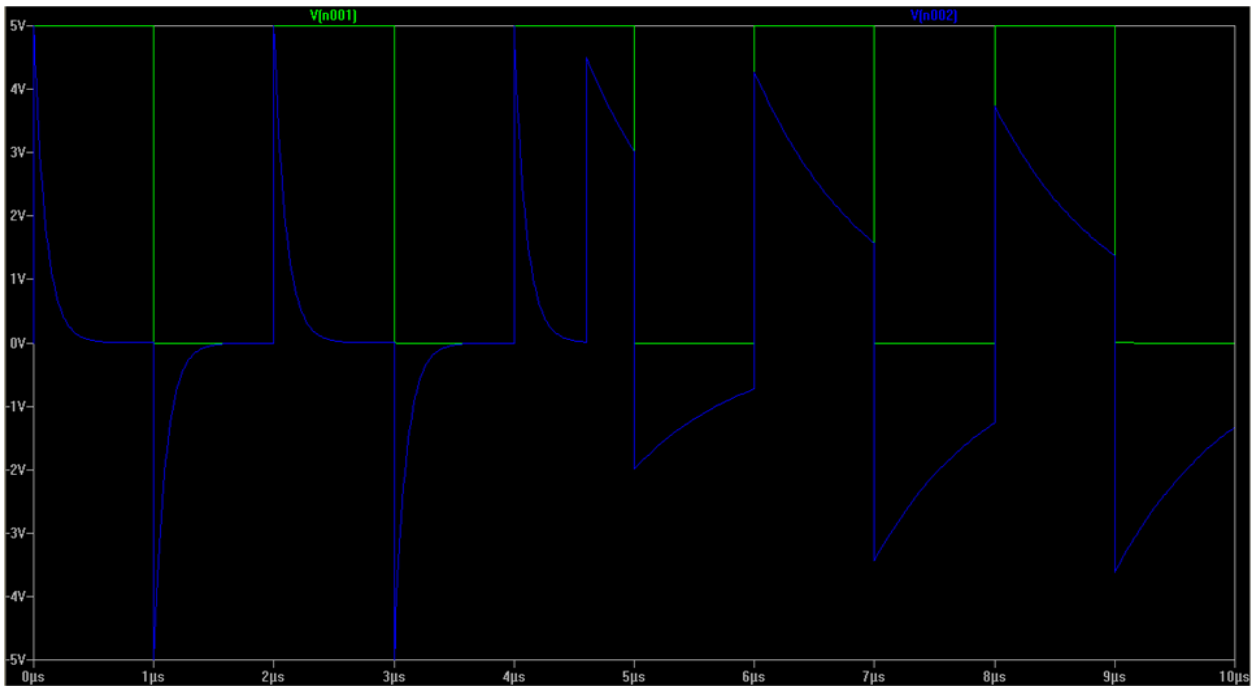

Figure 19. Output of an LR circuit with variable L switched at time 4.6 μsec

The inductor value is switched from 0.1 mH to 1 mH, at time 4.6 μsec. The circuit is as shown below –

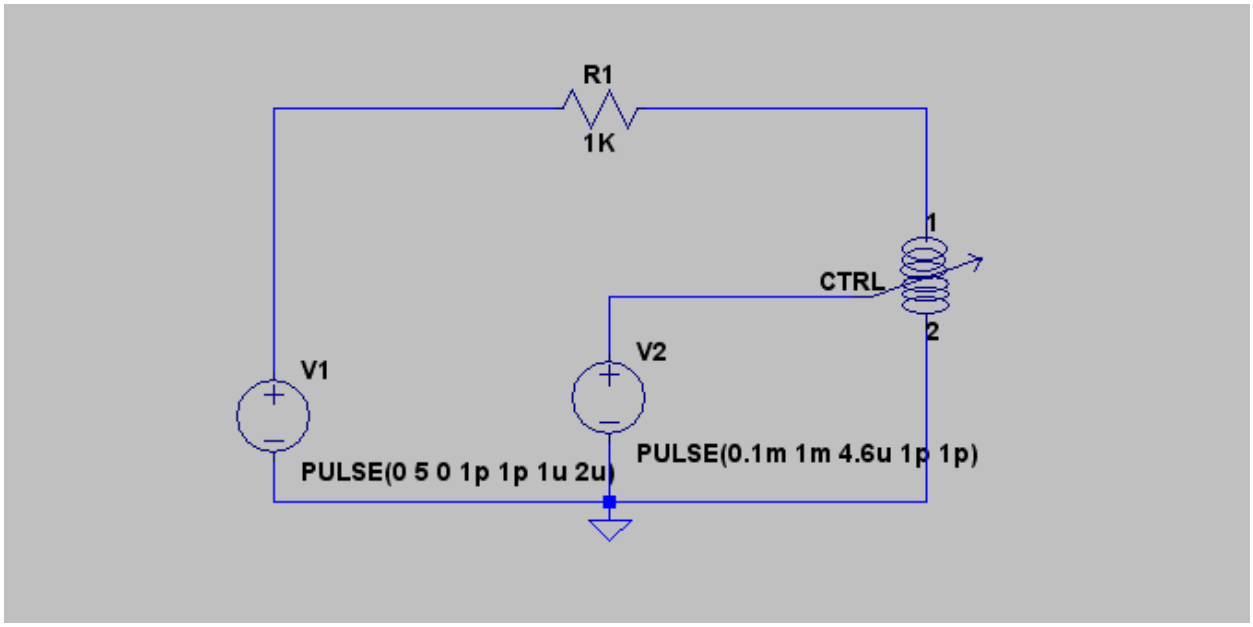

Figure 20. LR circuit with variable L

Again we note that the value of controlling voltage source assumes the values numerically equal to the inductance value to be achieved. The reason for this will be understood later when we explain the technique for implementing variable inductor.

4.2. General Idea about Variable Element Schemes

As already mentioned we plan to implement a lossless transmission line using a standard model. The static elements of the standard model would be replaced with the variable ones, just as we did in the above circuits. This structure involving variable elements would be consisting of two functionally different parts – the transmission line part, over which the signal or disturbance travels, and the controlling part which ensures proper switching in the L and C values in time.

These two sections, though working independently of each other, interact in a very well defined manner to produce the desired outcome. As we will see later the controlling section of the line can be seen as a black box, taking input as the currents and the voltages of the disturbances travelling on the line. It inherently needs these signals to check the present flux and charge over the elements, so that it can enforce the preservation of these quantities by forcing appropriate voltages and currents. The scheme is developed by bearing in mind the very basic necessity of preserving the charge over C and flux over L. Pictorially, this can be represented in a crude manner as shown here –

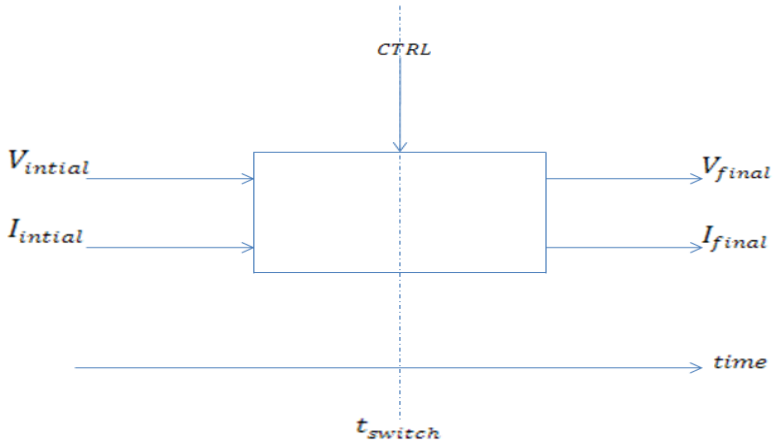

Figure 21. Pictorial representation of variable element scheme

Even though the scheme is continuously in action to produce any desirable switching function, it needs not only the controlling signal CTRL, but also the current signals over the transmission line. This means that even if the circuits function irrespective of the signal travelling on the line, we definitely need the presence of signal to testify its efficiency in preserving the charge and

flux over C and L, respectively. For example in a real world scenario, inductance could be varied by altering the current in the secondary winding of a transformer being used as an inductor [21][22]. Even though the controlling current is active, we need current in primary to measure the new inductance value. Thus signal on the actual transmission line is essential to have any observation and testify the success of the controlling circuit.

5. Spice Simulation

Simulator used – LTspice IV
Linear Technology, SwCAD III

5.1. Implementation of Variable Inductor

A static inductor maintains, the following relation between voltage and current across two nodes a and b of the circuit;

$$V_{ab} = L\frac{dI_{ab}}{dt},$$

where L is the inductance. Any arrangement which simulates such V-I relation across the nodes a and b, is essentially behaving as an inductor.

The above equation is the same as

$$I_{ab} = \frac{\int V_{ab}\,dt}{L}. \qquad (11)$$

The motive of rearranging the equation is to get it in the form of standard capacitor equation:

$$V = \frac{1}{C}\int I\,dt\,,$$
$$= \int I\,dt \text{ ....(for C = 1F)}$$

which is similar to numerator of RHS of eq^n.(11) except current I takes the place of V_{ab}. This is because electrical circuit implementation of integrals is most convenient using capacitors and current, hence we will mimic the voltage through current. Thus we can achieve the numerator of RHS of eq^n.(11) by forcing a current I numerically equal to V_{ab} through a 1F capacitor as shown in figure. (22), below. An 'arbitrary behavioral current source' BINT is forcing a current I through a 1F capacitor CINT. As mentioned earlier, the voltage V(INT) developed across the capacitor at node INT is the numerator of RHS of eq^n.(11) and hence eq^n.(11) becomes –

$$I_{ab} = \frac{V(INT)}{L} \qquad (12)$$

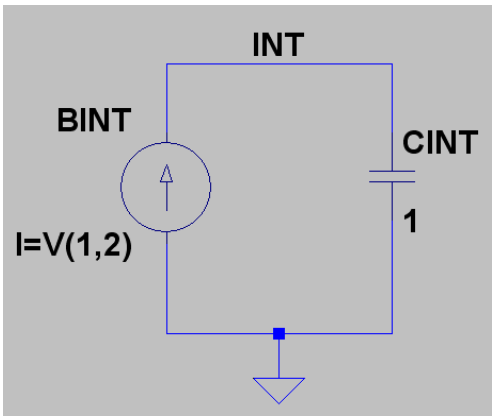

Figure 22. Integrating circuit for variable L scheme

As seen in figure. (22), the statement to mimic voltage through current is simply I = V(1,2), which is like equating two quantities with different units, which is not really true. It is worthwhile to mention at this point, that Spice do not need user to specify the unit of the quantity. It assumes the standard unit for the quantity defined by the standard symbol. For example, I is a standard symbol for current in Spice and hence Spice will automatically assume the standard MKS unit for it as Amperes. User just needs to specify the numerical value for the current, say, $I = 4$ which for Spice means 4 amps. Similarly, a statement like L = 300μ means inductance of 300μH. Instead of stating a numerical value we can also assign some variable whose value can be arbitrarily assigned and changed during execution. For example, a statement like L = V(CTRL), means inductance equal to the present voltage value at some node CTRL in the circuit. The unit is naturally assumed to be Henries. Implementing this in eq^n.(12), we get

$$I_{ab} = \frac{V(INT)}{V(CTRL)} \tag{13}$$

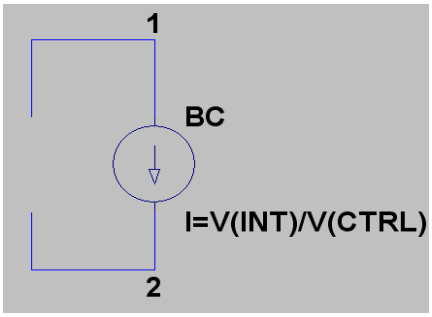

Figure 23. Current source implementing the inductor current

As seen in the figure (23) above, the current I_{ab} flowing across nodes a and b (designated as nodes 1 and 2 in figure (23) above) can be easily achieved and maintained in LTspice using an

inbuilt 'Arbitrary behavioral current source'. Such a current source maintains current through it specified by any arbitrary equation, thus enabling the current to be a function of independent variables and constants. The generalized syntax is –

$$I = F(\dots)$$

Examples: In figure (22), for current source BINT, $I = V(1,2)$, i.e. voltage across nodes a and b.

In figure (23), for current source BC, $I = \frac{V(INT)}{V(CTRL)}$, i.e. ratio of two node voltages.

As seen earlier, L = V(CTRL) which is the variable voltage at some node CTRL in the circuit. This way we can vary the inductance by altering the voltage at node CTRL. To be precise, the inductance is numerically exactly the same as node CTRL voltage.

To summarize, it starts with sensing the value of voltage across the inductor, V_{ab} and ends up adjusting the current through the inductor I_{ab}. The flux preservation demands adjustment of the inductor current depending on the variation in the inductance value, to preserve the product $L * I_{ab}$. Hence the black box discussed earlier in section 4.2, has an output of current I_{ab} while the inputs are V_{ab} and $V(CTRL)$. The net circuit for variable inductor is shown in figure (24) below.

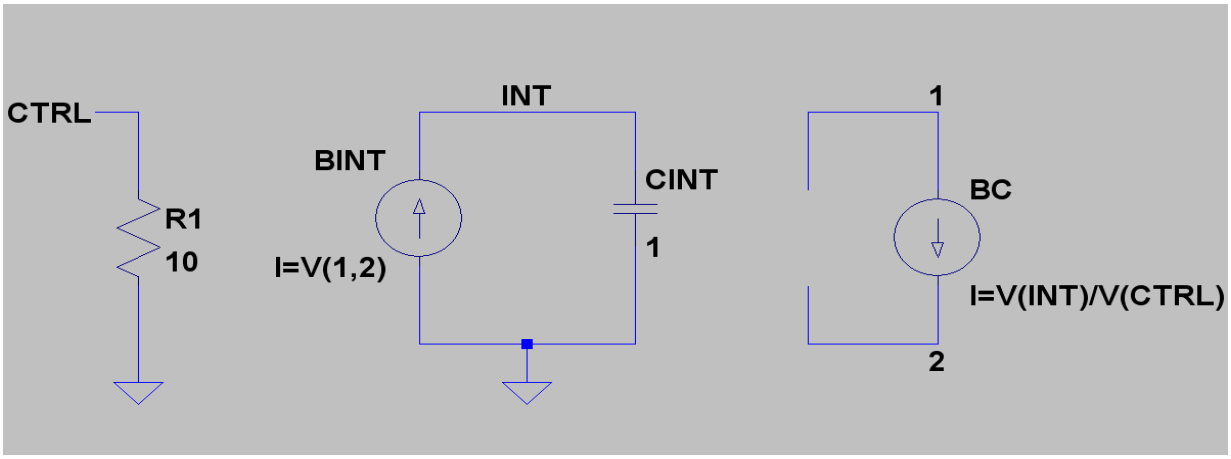

Figure 24. Variable inductor circuit

The above circuit ensures the essential flow of current I_{ab} through the branch connecting nodes a and b (designated as 1 and 2), having voltage V_{ab} across it, and related by equation (11). Thus the circuit essentially sees an inductor of value L = V(CTRL) connected between the nodes a and b. With this inductor assuming value L_1, we obtain

$$I_1 = \frac{1}{L_1}\int V_1 dt, \qquad \text{exhibiting material 1,}$$

while, switching the value to L_2 would give

$$I_2 = \frac{1}{L_2}\int V_2 dt, \qquad \text{exhibiting material 2.}$$

Since V(CTRL) is an independently controlled voltage, which can be set equal to any desired value, we can switch the value of L form L_1 to L_2, and switch the properties of the materials in time.

5.1.1. Spice Netlist

```
.subckt variable 1 2 CTRL
BC 1 2 I=V(INT)/V(CTRL)
BINT 0 INT I=V(1,2)
CINT INT 0 1
R1 CTRL 0 10
.ends variable
```

5.1.2. Variable Inductor: A Three-Port Device.

Symbol –

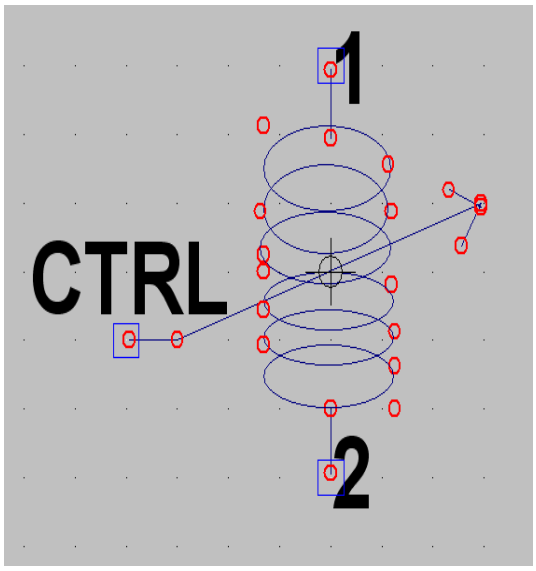

Figure 25. Symbolic representation of variable inductor circuit.

From the circuit in figure (24), and also from the above symbol we see that a variable inductor is a three-port device with two usual ports (port 1 and 2 in the above symbol) of a static inductor used to connect the device in the network, and a control port (CTRL in the above symbol) used as a switch/knob to switch the value of inductor. We also understand that the inductor value is same as the numerical value of voltage applied to this control port, which we mentioned in earlier section, too. For example, to obtain an inductor of 480 μH we need to apply a voltage value as 480 μV at CTRL port. We will later see how this technique is used to implement material substrates with dynamic material properties.

5.1.3. Reliable working of a Variable Inductor (Demonstration of Flux Preservation)

In section 4.1., we have already seen the circuits and their plots demonstrating the faithful working of a variable Inductor to produce results exactly similar to its static counterpart. Their ability to reproduce the effects of static element can be numerically verified for accuracy. Rather, we are more interested in the fact, as mentioned earlier too, that this scheme ensures the preservation of flux. A small discussion about this was done in the preceding section 4.1, and here we will demonstrate this graphically.

We know that for the variable inductor scheme, L = V(CTRL), numerically. Also the flux linkage of the device will be given by $\varphi = L * I_{ab} = V(CTRL) * I_{ab}$, numerically. For the LR circuit shown below, we have plotted the graph of the inductor current I_{ab} (Ix(x1:1) in the graph – green), and the flux $V(CTRL) * I_{ab}$ (Ix(x1:1)*V(n003) in the graph – blue). A sine voltage with a frequency of 100K is applied to the circuit and the simulation is observed for a period of 100 μsec. At time 50 μsec, the inductance in the circuit is made to switch from 1 mH to 10 mH, which is reflected by the immediate change in the inductor current, but the flux curve remains unchanged as expected. Note that the unit for the flux is shown as Watts, and not Weber or Tesla. This is because we have expressed the L value as voltage, and not in Henries as ideally should have been. Nonetheless we do observe the preservation of flux from the graph.

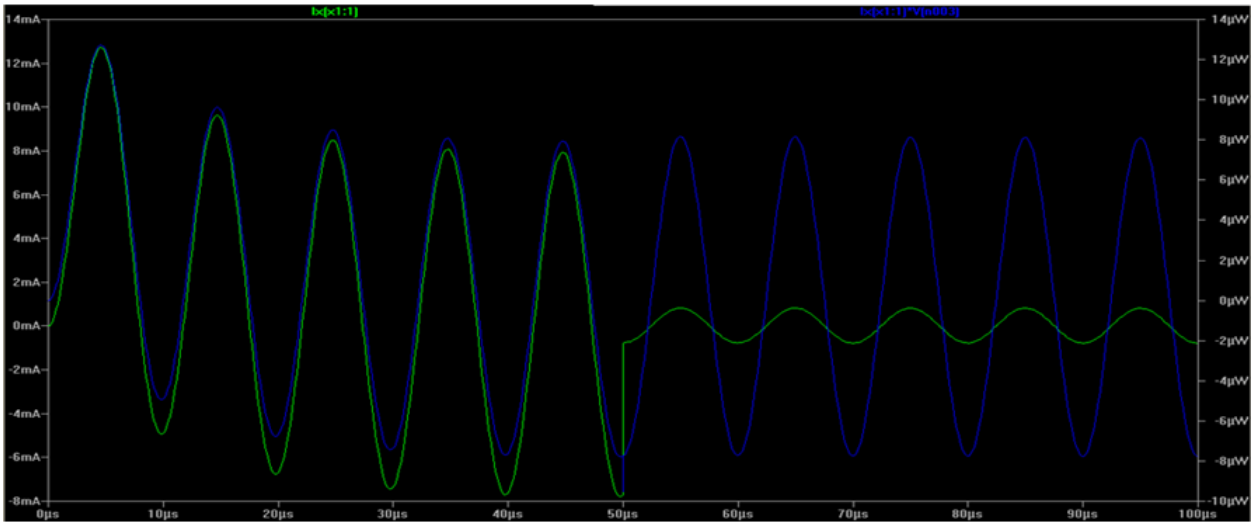

Figure 26. Demonstration of flux preservation with variable inductor technique

5.2. Implementation of Variable Capacitor in Spice –

The idea is exactly similar to that of the variable inductor. Again, the value of C in the capacitor equation will be specified by an independent control voltage.

A static capacitor C connected between nodes a and b in a circuit, maintains the following V-I relation between it –

$$I_{ab} = C\frac{dV_{ab}}{dt},$$

which is same as

$$V_{ab} = \frac{\int I_{ab}\,dt}{C}. \qquad (14)$$

The motive of rearranging the equation is to get it in the form of standard capacitor equation:

$$V = \frac{1}{C}\int I\,dt\,,$$
$$= \int I\,dt \quad \text{.....(for C = 1F)}$$

which is similar to numerator of RHS of eq^n.(14) except current I takes the place of I_{ab}. We can achieve the numerator of RHS of eq^n.(14) by forcing a current I numerically equal to I_{ab} through a 1F capacitor as shown in figure. (27), below. An 'arbitrary behavioral current source' BINT is forcing a current I through a 1F capacitor CINT. As mentioned earlier, the voltage V(INT) developed across the capacitor at node INT is the numerator of RHS of eq^n.(14) and hence eq^n.(14) becomes –

$$V_{ab} = \frac{V(INT)}{C} \tag{15}$$

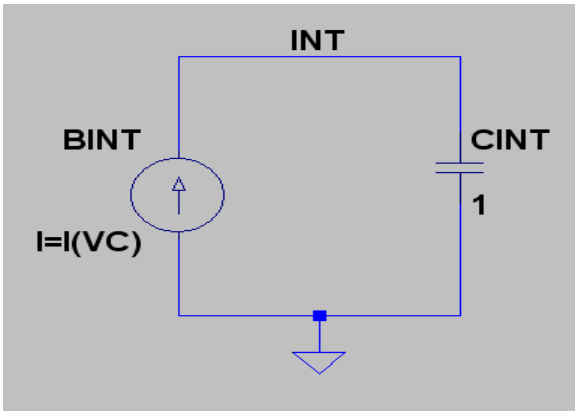

Figure 27. Integrating circuit for variable C scheme

The current seen in figure (27), above, I(VC) is the current through a voltage source VC connected in the branch joining nodes a and b. Here the voltage source is used as a current sensing device, which senses the current I_{ab}. Spice allows using a voltage source as a current sensing device if no voltage value or function is specified for it, as shown in figure (28). As natural with all current meters, the voltage drop across VC is zero. Just as we did in the case of variable inductor, we will assign the capacitance as a arbitrary variable voltage V(CTRL) occurring at some node CTRL, and can be altered as many times during execution. The capacitance value becomes exactly equal to the V(CTRL), while the units are naturally assumed to be in Farads.

$$V_{ab} = \frac{V(INT)}{V(CTRL)} \tag{16}$$

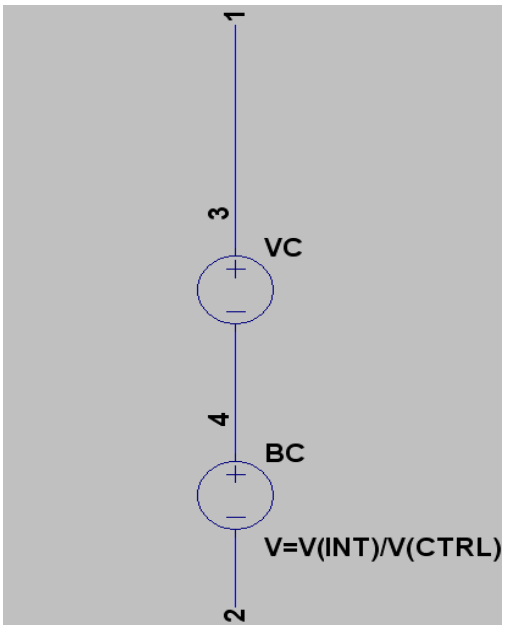

Figure 28. Current sensor and voltage source implementing capacitor voltage

As seen in the figure (28), above, the voltage V_{ab} across nodes a and b can be easily achieved and maintained in LTspice using an inbuilt 'Arbitrary behavioral voltage source'. Such a voltage source maintains voltage across it specified by any arbitrary equation, thus enabling the current to be a function of independent variables and constants. The generalized syntax is –

$$V = F(\dots)$$

Examples: In figure (28), for voltage source BC, $I = \frac{V(INT)}{V(CTRL)}$, i.e. ratio of two node voltages.

As seen earlier, C = V(CTRL) which is the variable voltage at some node CTRL in the circuit. This way we can vary the capacitance by altering the voltage on node CTRL. To be precise, the inductance is numerically, exactly, the same as node CTRL voltage.

To summarize, it starts with sensing the value of current through the capacitor, I_{ab} and ends up adjusting the voltage across the capacitor V_{ab}. The charge preservation demands adjustment of the capacitor voltage depending on the variation in the capacitance value, to preserve the product $C * V_{ab}$. Hence the black box discussed earlier in section 4.2, has an output of voltage V_{ab} while the inputs are I_{ab} and $V(CTRL)$. The net circuit for variable inductor is shown in figure (29) below.

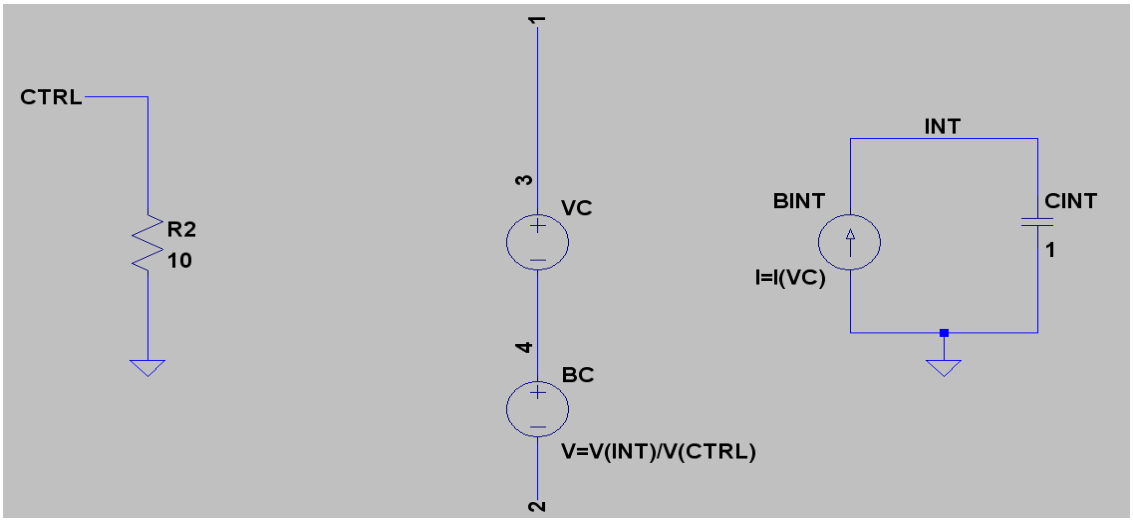

Figure 29. Variable capacitor circuit

The above circuit ensures the essential flow of current I_{ab} through the branch connecting nodes a and b, having voltage V_{ab} across it, and related by equation (14). Thus the circuit essentially sees a capacitor of value C = V(CTRL) connected between the nodes a and b. With this inductor assuming value C_1, we obtain –

$$V_1 = \frac{1}{C_1}\int I_1 dt, \qquad \text{exhibiting material 1,}$$

While, switching the value to C_2 would give –

$$V_2 = \frac{1}{C_2}\int I_2 dt, \qquad \text{exhibiting material 2.}$$

Since V(CTRL) is an independently controlled voltage, which can be set to any desired value, we can switch the value of C form C_1 to C_2, and switch the properties of the materials in time.

5.2.1. Spice Netlist –

```
.subckt variable 1 2 CTRL
BC 4 2 V=V(INT)/V(CTRL)
BINT 0 INT I=I(VC)
CINT INT 0 1
R2 CTRL 0 10
VC 1 4
.ends variable
```

5.2.2. Variable Capacitor: A Three-Port Device

Symbol –

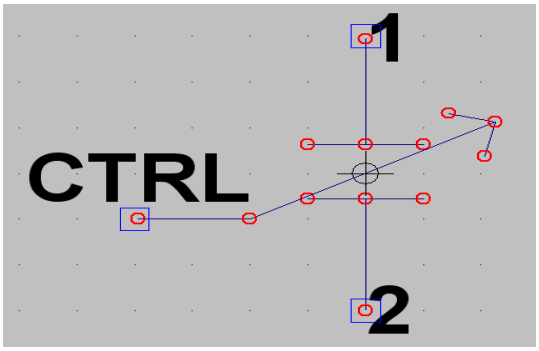

Figure 30. Symbolic representation of the variable capacitor circuit

From the circuit in figure (29), and also from the above symbol we see that the variable capacitor is a three-port device with two usual ports (port 1 and 2 in the above symbol) of static capacitor used to connect the device in the network, and a control port (CTRL in the above symbol) used as a switch/knob to alter the value of capacitor. We also understand that the capacitor value is same as the numerical value of voltage applied to this control port. For example, to obtain a capacitor of 0.48 pF we need to apply a voltage value as 480 pV at the CTRL port.

5.2.3. Reliable Working of a Variable Capacitor Circuit (Demonstration of Charge Preservation) –

Similar to the demonstration of the flux preservation in the case of inductor, here we demonstrate the success of the variable capacitor scheme in preserving the charge over the capacitor, with varying the value of capacitance. We know that the capacitance C = V(CTRL) numerically, and also that the charge over a capacitor is given by $Q = C * V_{ab} = V(CTRL) * V_{ab}$.

For the RC differentiator circuit shown below, we have plotted the graph of the capacitor current V_{ab} (V(N001,N002) in the graph – green), and the charge $V(CTRL) * V_{ab}$ (V(N001,N002)*V(n004) in the graph – blue). A sine voltage with a frequency of 100K is applied to the circuit, and the simulation is observed for a period of 100 μsec. At time 50 μsec, the capacitance in the circuit is made to switch from 0.01 μF to 0.1 μF, which is reflected by the immediate change in the capacitor voltage, but the charge curve remains unchanged as expected. Note that the unit for the charge is shown as V^2, and not Coulomb. This is because

we have expressed the C value as voltage, and not as Farads, as ideally should have been. Nonetheless we do observe the preservation of charge from the graph.

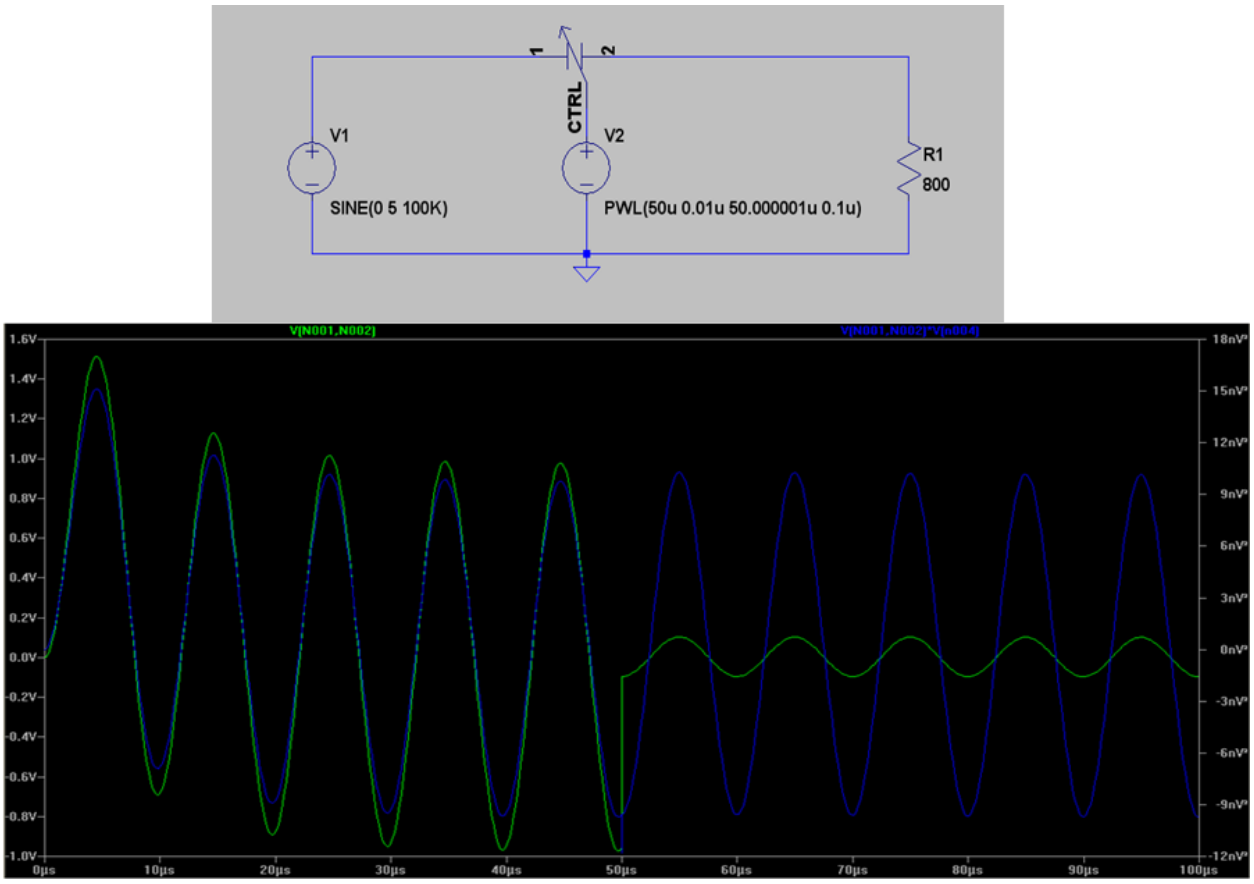

Figure 31. Demonstration of charge preservation with variable capacitor technique

5.3. Transmission Line Unit Using Variable L and Variable C

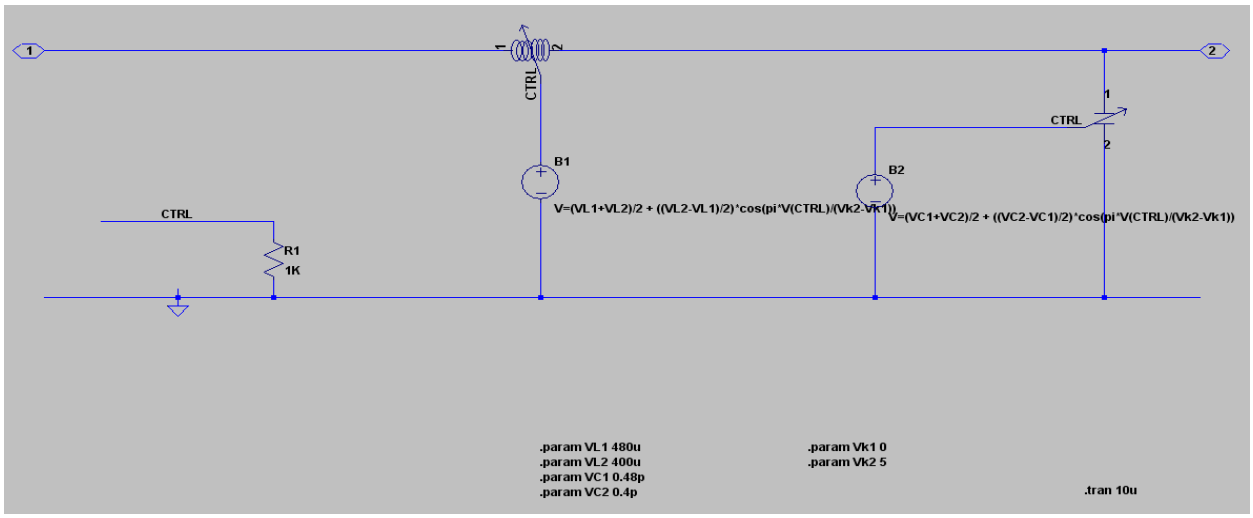

Figure 32. A single LC unit of a transmission line with variable elements

Once we have our variable inductor and capacitor ready, we connect them in a standard transmission line structure. One such unit of a transmission line is shown above in figure (32). There are two independent voltage sources B1 and B2, each controlling the values of variable inductor and capacitor individually. Our application demands switching of the inductor and capacitor values between two discrete levels, in order to achieve two distinct materials. For this we will need to set parameters for the two materials.

Material 1	Material 2
$L_1 = 480\ \mu H/\text{m}$	$L_2 = 400\ \mu H/\text{m}$
$C_1 = 0.48\ pF/\text{m}$	$C_2 = 0.4\ pF/\text{m}$

To switch between material 1 and 2, we need to switch the voltage at the CTRL port of the variable inductor between $400\mu V$ and $480\mu V$. This is achieved by an 'arbitrary behavioral voltage source' (B1 in figure 32, above), which produces the two desired voltage levels. The equation for voltage by B1 is given as –

$$V = \frac{(VL1+VL2)}{2} + \frac{(VL2-VL1)}{2} cos\left(\pi * \frac{V(CTRL)}{(Vk2-Vk1)}\right), \quad (17)$$

where, $VL1$ = 480 μV, & $Vk1$ = 0 V
$VL2$ = 400 μV, & $Vk2$ = 5 V and $V(CTRL)$ is an independent voltage.

$V(CTRL)$ acts as a switch to control the voltage of B1 and hence the inductor value. $V(CTRL)$ can be switched between the value of $Vk1$ and $Vk2$, i.e. 0 and 5.

When $V(CTRL) = 0\,V$ ➔ $V = VL2 = 400\mu V$ ➔ $L = L_2 = 400\mu H$
When $V(CTRL) = 5\,V$ ➔ $V = VL1 = 480\mu V$ ➔ $L = L_1 = 480\mu H$

Similar to the inductors, we need to switch the voltage at the CTRL port of the variable capacitor between $0.4pF$ and $0.48pF$. This is achieved by an 'arbitrary behavioral voltage source' (B2 in figure 32, above), which produces the two desired voltage levels. The equation for voltage by B2 is given as –

$$V = \frac{(VC1+VC2)}{2} + \frac{(VC2-VC1)}{2} cos(\pi * \frac{V(CTRL)}{(Vk2-Vk1)}) \quad (18)$$

Where, $VC1$ = 0.48 pF, & $Vk1$ = 0 V
$VC2$ = 0.40 pF, & $Vk2$ = 5 V

With $V(CTRL)$ taking values as $Vk1$ and $Vk2$, we obtain the following
When $V(CTRL) = 0\,V$ ➔ $V = VC2 = 0.40pV$ ➔ $C = C_2 = 0.40pF$
When $V(CTRL) = 5\,V$ ➔ $V = VC1 = 0.48pV$ ➔ $C = C_1 = 0.48pF$

Notice that V(CTRL) is the common control parameter occurring in the equations for voltages of B1 and B2, enabling a single control circuit for switching of L and C. This ensures simultaneous switching of the variable L and C, which is absolutely essential for faithful change between material 1 and 2.

Also, the voltages are cosine functions of V(CTRL), which provides a smooth transition of B1 and B2 voltages and hence the inductor and capacitor values. Avoiding abrupt transitions minimizes any high frequency components which could create distortions even at lower operating frequencies. This also means there will be some inertia maintained in the system, which can almost be neglected. This is because even the highest frequencies of operation do not surpass the MHz range, while the switching signal rise and fall at 1 $psec$ duration.

Referring to the circuit above in figure (32), we find three ports for this section – input port <1>, output port <2>, and the CTRL port. This three port network forms a single unit of the transmission line, and can be symbolically represented as shown below in figure (33)

Symbol –

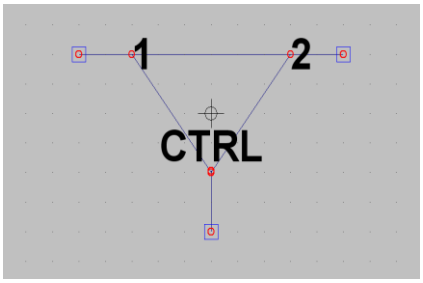

Figure 33. Symbolic representation of an LC unit of a transmission line

In the disicussion above, the value of L and C are expressed per meter length, which means one such LC unit consisting of 1 L and 1 C of the specified values, correspond to 1 meter length of space. Hence the length of the network with many such 3-port units cascaded together would exactly be equal to the number of units put together and measured in meters – l units cascaded together would measure l meters in length.

5.3.1. Spice Netlist

```
.subckt variablelc2 1 2 CTRL
XX1 1 2 N002 variablel
XX2 2 0 N001 variablec
R1 CTRL 0 1K
B1 N002 0 V=(VL1+VL2)/2 + ((VL2-VL1)/2)*cos(pi*V(CTRL)/(Vk2-Vk1))
B2 N001 0 V=(VC1+VC2)/2 + ((VC2-VC1)/2)*cos(pi*V(CTRL)/(Vk2-Vk1))
.param VL1 480u
.param VL2 400u
.param VC1 0.48p
.param VC2 0.4p
.param Vk1 0
.param Vk2 5
.ends variablelc2
```

5.4. Material Substrate modelled as a Transmission Line

In absence of the CTRL port, we would have the standard LC unit of a lossless transmission line with static line parameters. The addition of port CTRL allows control for parameter variations and hence suits our demand of material-switching in time. Many such three port units would be connected in series to form a single material substrate. For the entire material substrate to switch its properties at the same time instant we need to provide the V(CTRL) signal

simultaneously to all the units comprising the material. This needs CTRL ports of all such LC units to be connected in parallel to a common controlling circuit, as is shown below –

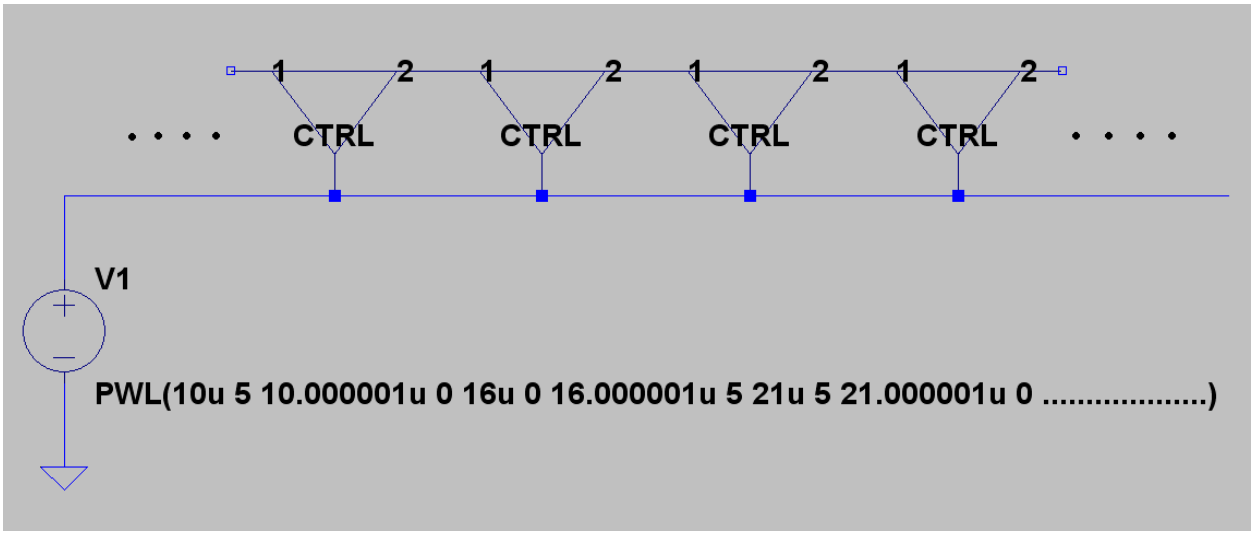

Figure 34. Transmission line section with variable LC units

5.5. Controlling Circuit for the CTRL Ports

The voltage source V1 in figure (34) above is an integral part of the control circuit, which takes care of the proper timings as prescribed by the specifications of the checkerboard.

For n = 0.5, and the temporal period of the checkerboard equal to 10 μsec, we need V1 to generate a square wave of amplitude 5V (since Vk2 – Vk1 = 5V), 50 % duty cycle and period of 10 μsec. The waveform shown below satisfy these requirements, with rise and fall time of 0.000001 μsec or 1 $psec$.

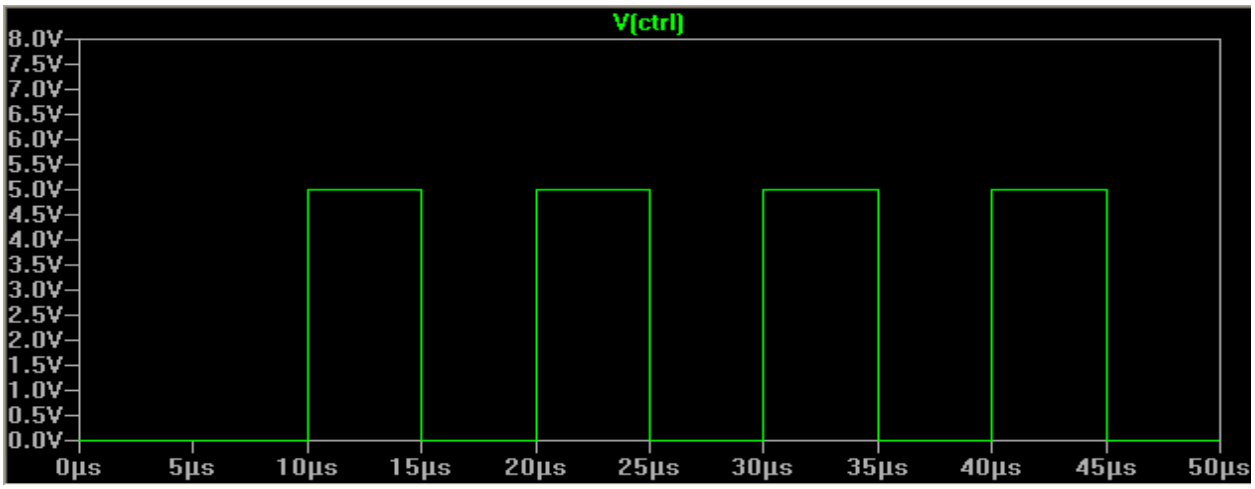

Figure 35. An example of a controlling signal

5.6. Practical Constraints Observed in the Simulation of a Transmission line

So far we have made the basic ingredients and the recipe ready to construct an actual transmission line in Spice. At this point we may ask ourselves a few important questions:

- ➔ What would be the total length spatially and temporally of the checkerboard structure?
- ➔ How many LC units would go in to achieve this desired length?
- ➔ What is the frequency that we may prefer to operate the system at?

All these question are not independent, rather they are interrelated and their answers need to be obtained in a holistic fashion. In an effort to answer them, there appeared to be practical contraints involved in the construction of a checkerboard. Let us try to see in this section what are they, and how they arise.

While answering the first question, we need to consider the fact that a single LC unit is a complex structure though it looks pretty simple and concise in its symbolic form. For better observations of the signal travelling along the transmission line, we may want to go with many periods in space and time. But the checkerboard being a 2D structure on paper, the calculation complexity squares up, putting a heavy load on the computing system. With an average power personal laptops, it was found to be very difficult to manage large lengths of checkeroard.

What if we try to keep the structure small? This would need smaller values of L and C per unit length. This looks fine until we start thinking about the operating frequency, since smaller values of L and C mean higher speed of the wave in the material substrates. At these higher speeds we find it difficult to incorporate one full or even half a cycle in the material substrate, as the leading egde tends to move out of the material before the trailling end is into it. Now to

get a solution to this, we can think of working with shorter wavelengths, or higher frequencies. This is not so good as it looks, since large distortions at higher frequencies are observed, making the collected data unimpressive. The reason for this lies in the theory of transmission line. In the standard model of transmission line, we define the L and C as distributed parameters. The smaller are the values of L and C per unit lengths in comparison to the operating wavelengths, better is the line modelled. At higher operating frequencies, our L and C start appearing as lumped rather than distributed, creating distortion in the output.

So there is a tradeoff between all the parameters to select. The effort started with a trail and error method, starting with higher frequencies trading down to lower ones, while moving higher in the lengths of checkerboard from few tens of LC units to reach a large number of 6000, while the starting frequency provided by the source had to be kept as low as 100K. The complete structure with the LC units and its description is shown in the next section.

5.7. Physical Construction of the Checkerboard in Space

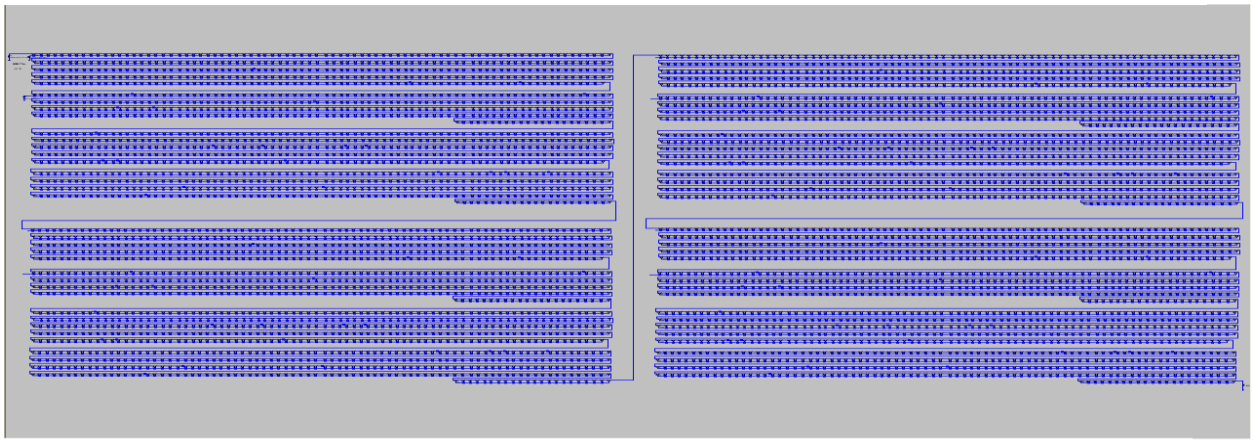

Figure 36. Physical construction of checkerboard

In the above structure, we observe 8 spatial periods of checkerboard, each period consisting of two material sustrates of unqual lengths. We can decide on the length of material sections based on the value of m and the total spatial period we desire in the real space. As an example, for a length of δ = 741 meters as spatial period, and m = 0.4615 we obtain the following –

Length of material one = m* δ = 0.4615*741 = 342 units
Length of material two = (1 – m)* δ = (1 – 0.4615)*741 = 399 units.

This difference in length is clearly apparent in the above figure (36) in each period. Apart from this length difference there is no physical difference in the two materials, since they consist of same LC units. In such a case what makes the two materials functionally different is the value of

L and C, which is controlled by the V(CTRL) signal. This means for material 1 to have parameter values as L1, C1, V(CTRL) would need to be 0, and at same time material 2 needs to have V(CTRL) value to be 5V so as to take the parameter values as L2, C2. Thus the controlling signal for each material is the inverted copy of the other as shown in figure (37) below along with their sources –

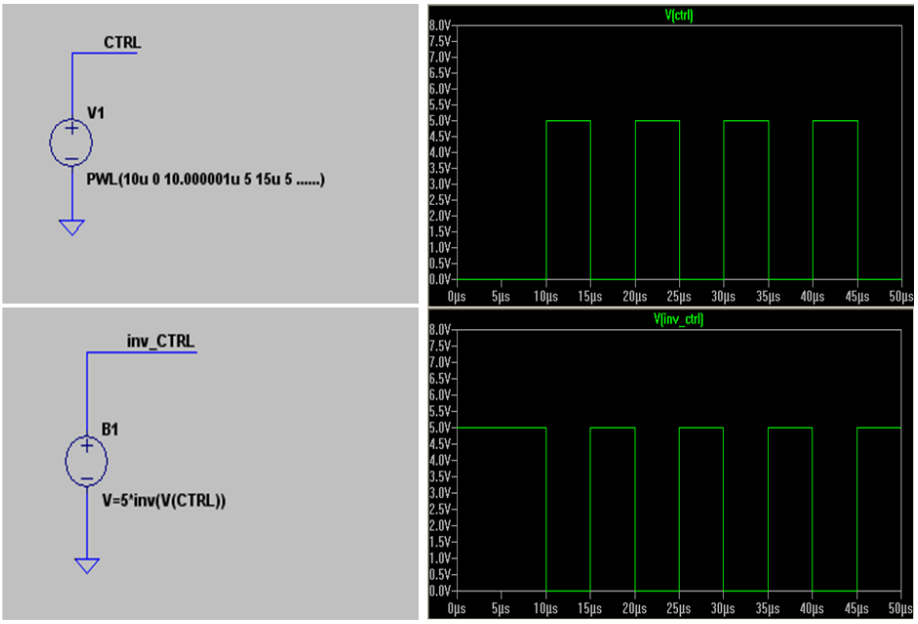

Figure 37. Controlling circuits with their outputs for two different materials

The signal V(CTRL) is provided to the first 399 cells, while the inverted control signal V(inv_ctrl) is provided to the remaining 342 cells in that spatial period, making them behave as two different materials at any given instant of time.

For time interval before 10usec, V(CTRL) = 0V provided to the first 399 cells. Therefore from equation (13) and (14), we see that for the first 399 cells $L = 400\mu H/m$ and $C = 0.4pF/m$. Hence the phase velocity in this medium and the wave impedance are given as –

$$v_2 = \frac{1}{\sqrt{(400\mu H)(0.4pF)}} = 7.9056942 \times 10^7\, m/s$$

$$\gamma = \sqrt{\frac{400\mu}{0.4p}} = 31.622777K$$

Similarly with V(int_CTRL) = 5V provided to next 342 cells, the phase velocity and the wave impedance of the wave in this material are given as –

$$v_1 = \frac{1}{\sqrt{(480\mu H)(0.48pF)}} = 6.5880785 \times 10^7\, m/s$$

$$\gamma = \sqrt{\frac{480\mu}{0.48p}} = 31.622777K$$

These figures reiterate the fact that the wave impedance in both the materials is same, while the phase velocities are different. Phase velocity in material 2 is greater than that in material 1. This is also obvious as in the given time duration of 0 to 10 μsec, the length of material 2 is greater than that of material 1, thus to accommodate the entire wave train of material 2 in shorter material 1, it has to shrink in size. This shrinking of size is due to low velocity of the leading edge of wave train in material 1, while high velocity of the trailing edge in material 2. Thus we see how these figures reassure us of the wave shrinking as the wave move from material 2 to material 1 across spatial boundary. This effect can be seen graphically later when we provide a plot of wave signal against space, as the wave travels through it.

5.8. Transmission Line Simulation

Let us summarize the system parameters discussed so far –

Length of each unit of transmission line = 1m
Number of units over spatial period $z = 0\ to\ z = m\delta$: 342
Number of units over spatial period $z = m\delta\ to\ z = \delta$: 399

Inductances and capacitances per meter of the transmission line are –
$L_1 = 480\ \mu H$/m
$C_1 = 0.48\ pF$/m
$L_2 = 400\ \mu H$/m
$C_2 = 0.4\ pF$/m

The spatial and temporal period and the velocities of the wave are –
$\delta = 399 + 342 = 741\ m$
$\tau = 5 + 5 = 10\ \mu sec$
$v_1 = \frac{1}{\sqrt{(400\mu H)(0.4pF)}} = 7.9056942 \times 10^7\, m/s$
$v_2 = \frac{1}{\sqrt{(480\mu H)(0.48pF)}} = 6.5880785 \times 10^7\, m/s$

The checkerboard parameters are –
$m = 342/(399 + 342) = 0.4615$
$n = 5/(5 + 5) = 0.5$

We know that the spatial period extends to $\delta = 741\ m$ of space, while temporal period is $\tau = 10\ \mu sec$. Thus using the standard MKS units of space and time gives the velocities of waves in two materials as obtained above. As we had discussed earlier, the characteristic path

of the waves are not really dependent on the absolute values of spatial and temporal periods, but on combined effect of the arrangement of the materials and temporal switching represented by the parameters m and n respectively. Hence for a generalized argument we would not refer to the absolute values in meters and sec, but will define the spatial period on the checkerboard always equal to 1 unit distance, while temporal period of 1 unit time. For example in our case, spatial period of 741 meters is equal to 1 unit checkerboard distance, and 10usecs of time is equal to 1 unit checkerboard time. This scaling results into new values of phase velocities, given as:

$$a_1 = v_1 \frac{\tau}{\delta} = 1.067$$
$$a_2 = v_2 \frac{\tau}{\delta} = 0.8891$$

Above circuit consists of 8 spatial periods, each period having 741 units, hence the total number of units = 8 x 741 = 5928.

6. Results

6.1. Time Plot

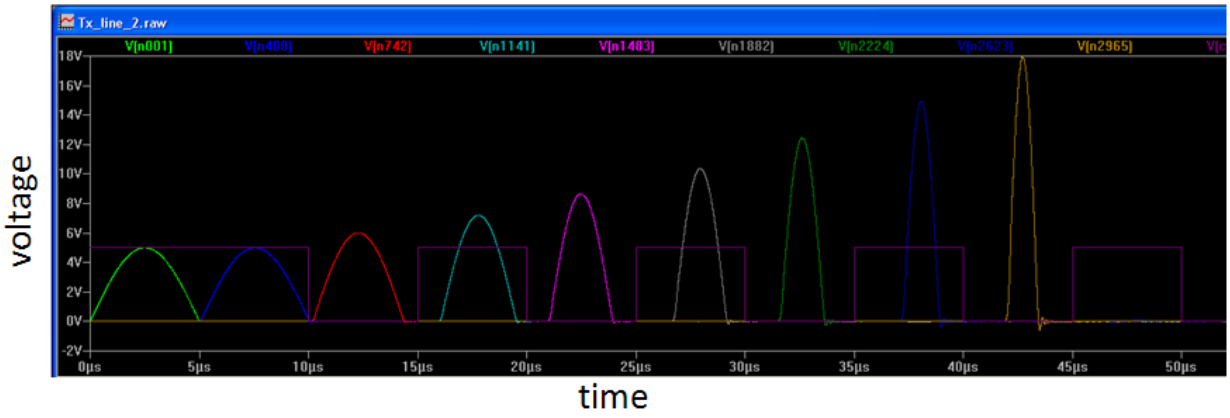

Figure 38. Time plot of voltage over transmission line at various nodes

The source sends half a cycle of sin wave, of frequency 100K. The square wave, which is the temporal switching signal V(CTRL) indicates those instances when medium change took place. It's clear that after every temporal switching, the wave frequency increases, and also the amplitude. The frequency and amplitude increment is in agreement with the theoretical estimates, based on the equation described earlier in this report. Also, some distortion is observed as the frequency tends to increase. This is because, at higher frequencies, the discreet components become comparable to the wavelengths, and the material is no longer seen as homogeneous. Operating at lower frequencies ensure no distortion or reflections.

To quantitatively verify the success of the system, we make use of the relations obtained by F. R Morgenthaler [17]. According to his work, the relation between initial and final voltage after temporal switching is given as

$$\text{Gain} = \frac{V_2}{V_1} = \frac{\varepsilon_1}{\varepsilon_2} = \frac{\mu_1}{\mu_2} = \frac{L_1}{L_2} = \frac{C_1}{C_2} .$$

In our case, the ratio L1/L2 = 480/400 = 1.2 or C1/C2 = 0.48/0.40 = 1.2. Clearly after k temporal switchings, we must observe the voltage peak to be

$$V_k = (1.2)^k V_1.$$

From the plot we observe that there are 7 temporal switchings before the final peak, hence k = 7 and the original source generates a voltage of 5 V, hence V_1= 5V.

Therefore, $V_7 = (1.2)^7 * 5 = 17.915\, V.$

This is exactly the value that we observe for the last peak in the above plot. This is an evidence for the accurate working of the system as predicted by the theory.

6.2. Verifying the Effects of the Structure Being On/Outside the Plateau

Here we experiment by changing the value of n, the structural parameter for checkerboard associated with temporal period, and seeing its effect on the output of the system. From the earlier shown result, we already know that the value of n = 0.5 keeps the system very much on plateau. Here is one more graph with n = 0.5, with more peaks observed.

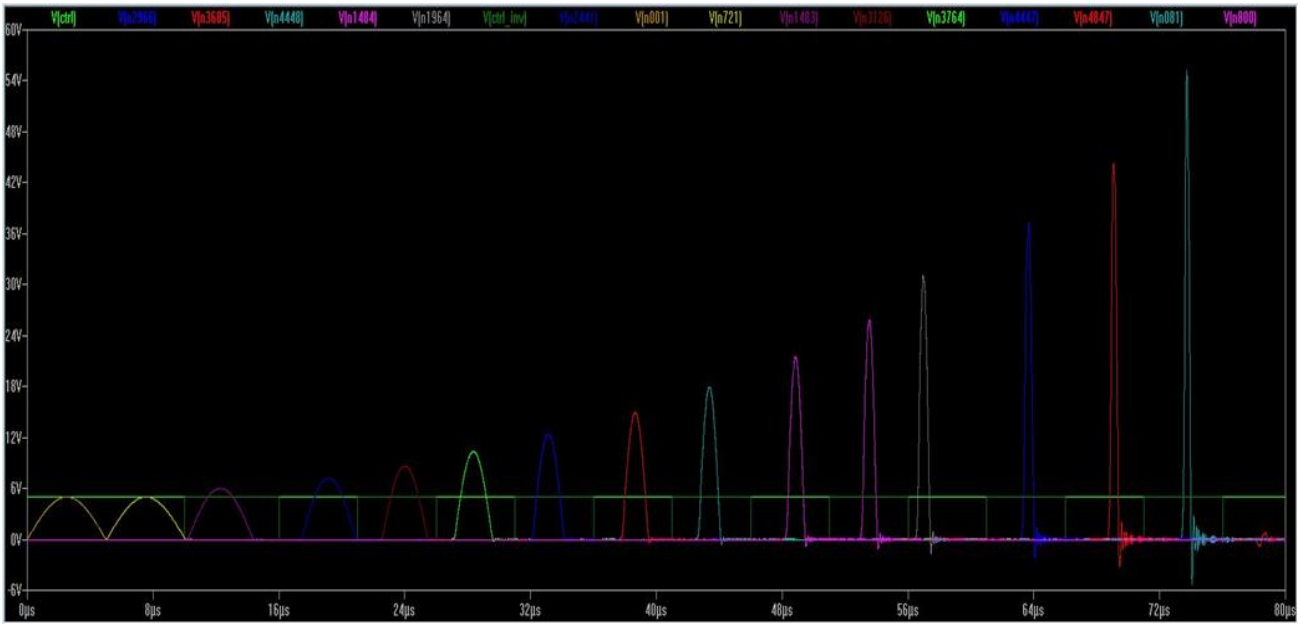

Figure 39. Time plot with n = 0.5

Let us again obtain the value of k^{th} peak using Morgenthaler's equations.

$$V_{13} = (1.2)^{13} * 5 = 53.4966\, V.$$

Clearly we see that the above graph still in accordance with the expected theory [18][16][17]. Now, we will vary the value of n and check if still we get the same results. The equation giving the condition for structure being on plateau is given as [18]

$$\frac{a_1\tau+\left(1-\frac{a_1}{a_2}\right)m-\delta}{a_1-a_2} \leq n \leq \frac{a_1\tau+\left(1-\frac{a_2}{a_1}\right)m-\delta}{a_1-a_2},$$
$$\frac{m-a_2\tau+\frac{a_2}{a_1}(\delta-m)}{a_1-a_2} \leq n \leq \frac{m-a_2\tau+\frac{a_1}{a_2}(\delta-m)}{a_1-a_2}.$$

Calculating with the values of other checkerboard parameters, we find the condition on n to be

$$0.19119 \leq n \leq 0.88090.$$

For n = 0.6

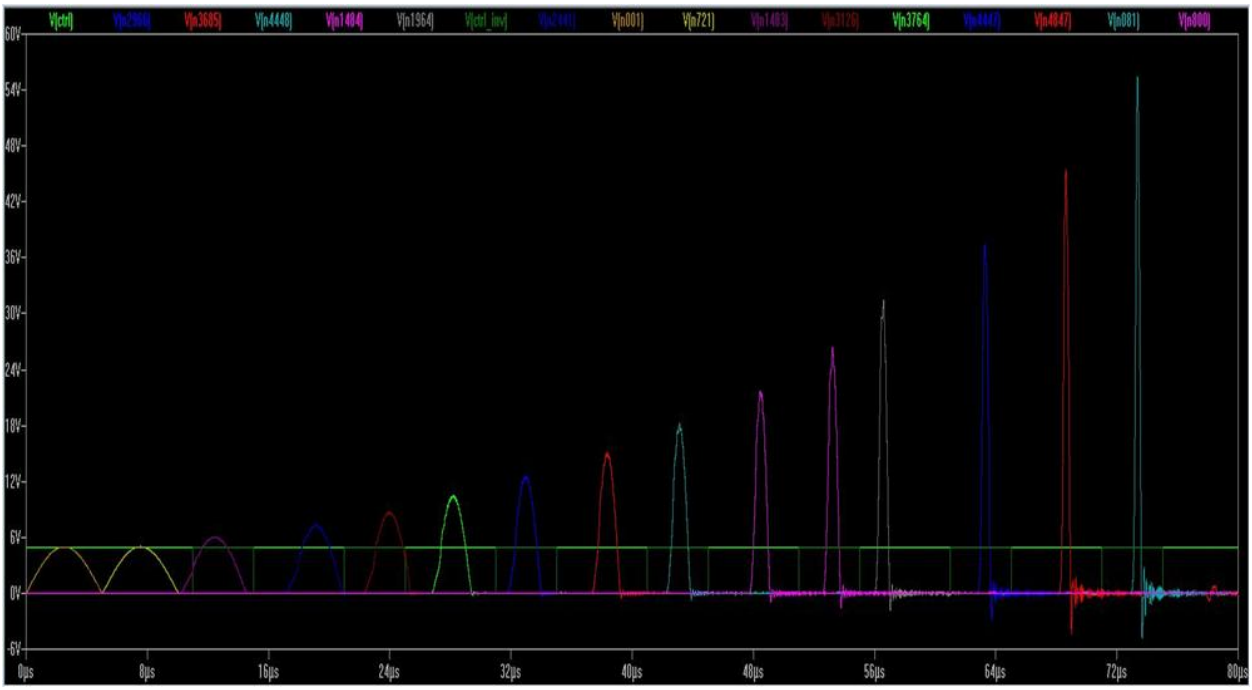

Figure 40. Time plot with n = 0.6

For n = 0.75

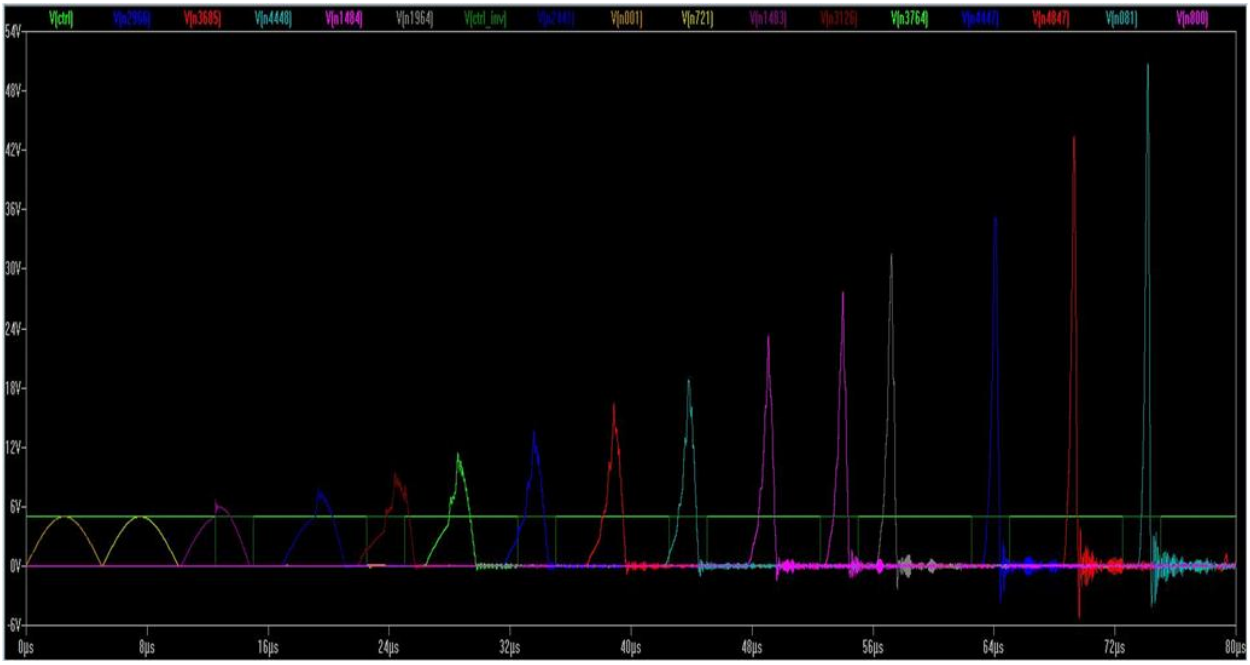

Figure 41. Time plot with n = 0.75

These plots are all in accordance with the expected behavior. We also note that irrespective of what value of n we select, the peaks always corresponds to same values, indication the system is on plateau and approaching the stable limit cycle.

Now, let us try to move away from the plateau, by selecting n values outside the range permissible by the plateau definition. We would select n values beyond 0.89 and further, as shown-

For n = 0.9

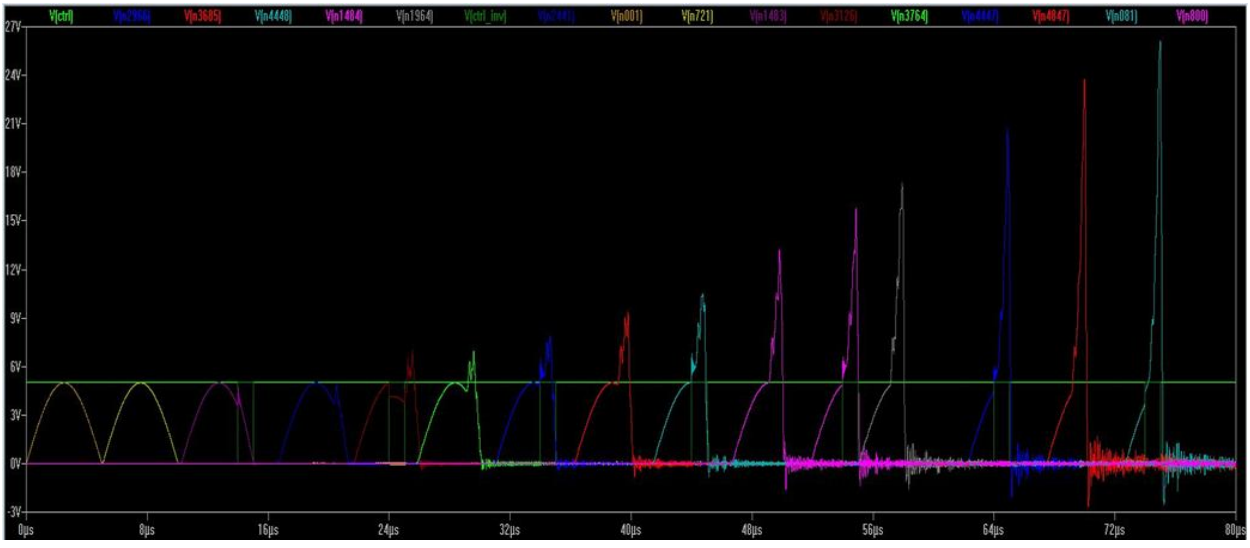

Figure 42. Time plot with n = 0.9

Note the highest peak value for this graph. This is clearly not in accordance with the Morgenthaler equation, and serves as clear indication of deviation from the stable limit cycle. This is just as expected since we have crossed the upper limit on n for a stable limit cycle. Let us have one more value of n beyond this limit and see the result –

n = 0.95

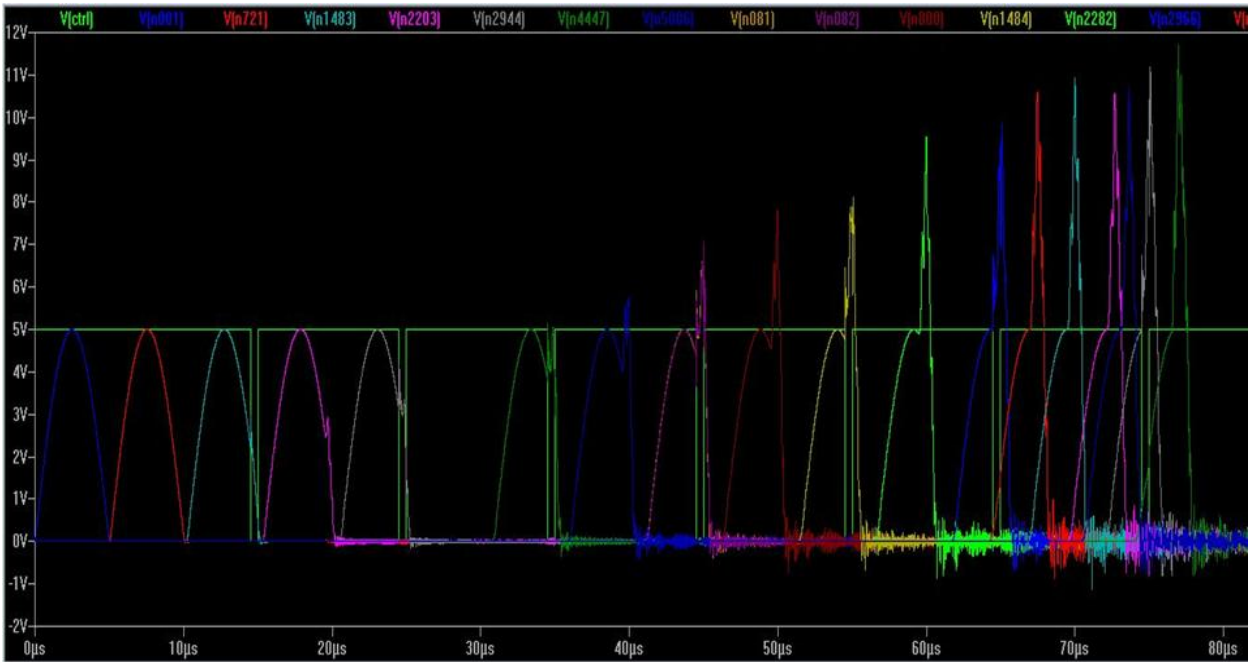

Figure 43. Time plot with n = 0.95

Note how the highest peak voltage fails further to reach the expected value, indicating we are further away from the stable limit cycle.

These results are convincing enough to conclude about the expected behavior of the system, and encourage us to put out hands to actual construction of a material substrate demonstrating similar behavior in real world too.

6.3. Space Plot

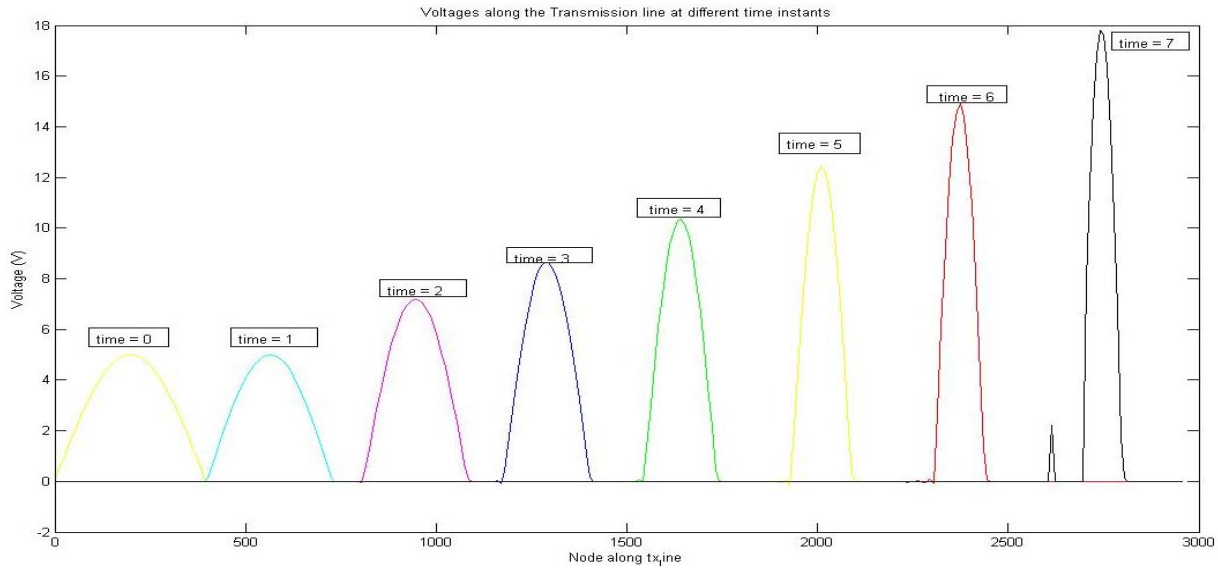

Figure 44. Plot of voltage over transmission line against space

Spice by default always provides time plots, and we need a space plot to verify the contraction of the wave as it travels in space. For this, we had to extract the data from the .raw file from Spice to Matlab [24]. In Matlab, we obtain a 2D matrix with voltage at each node for each time instant. To obtain space plot, we need to plot voltage at all time instants at a fixed given node. All such nodes are represented along the x-axis in the figure (44). The voltage was measured on different points along the transmission line, at different times for n = 0.5 and k = 7 switchings, as the wave travelled through it. Note that the peak after first switch is missing which should have taken the value $V_1 = (1.2)^1 * 5 = 6V$. This peak is seen in the time plots. The above graph demonstrates wave contraction in space. The voltage amplitude is increased as expected from the theory. The structure appears to be on a plateau and approaching limit cycle.

7. Future Work

The results obtained from the simulations though are limited by the computational capacity of the processors, nonetheless do suggest correspondence to the results obtained from numerical analysis, carried our earlier. This is encouraging enough to make us take the next step of actual construction of such spatio-temporal material composite. Clearly, Spice simulation has only been able to confirm the principle of working, and do not help us really to start with the real implementation. The method employed in Spice by no means can directly be transferred to hardcore construction. The technique of voltage and current manipulation to preserve the flux and charges at temporal switching, is not meant for real world. In nature these preservations are naturally obeyed by the elements given their physics. Thus we are supposed to make use of

these natural phenomenon to observe the energy accumulations and wave contractions, rather than forcing them. For this we need actual elements offering inductance and capacitance, and some means of modulating their values. There are various hurdles in the engineering of dynamic materials based on the transmission line models. In this section we will describe the possible problems that could be encountered in the engineering process and suggest certain approximate solutions for them.

The biggest problem in the engineering of above idea is to make available inductances and capacitances variable in time. To understand this better, let us try to see the table (1), below, which show the inductance formulas for certain simple inductor constructions in air [25].

Inductance of simple electrical circuits in air

Type	Inductance / μ_0	Comment
Single layer solenoid[5]	$\frac{r^2N^2}{3l}\left\{-8w+4\frac{\sqrt{1+m}}{m}\left(K\left(\frac{m}{1+m}\right)-(1-m)\,E\left(\frac{m}{1+m}\right)\right)\right\}$ $=\frac{r^2N^2\pi}{l}\left\{1-\frac{8w}{3\pi}+\sum_{n=1}^{\infty}\left(\frac{1\cdot 3\ldots(2n-3)}{2\cdot 4\cdot 6\ldots 2n}\right)^2\frac{2n-1}{2n+2}2^{2n+1}(-1)^{n+1}w^{2n}\right\}$ $=\frac{r^2N^2\pi}{l}\left(1-\frac{8w}{3\pi}+\frac{w^2}{2}-\frac{w^4}{4}+\frac{5w^6}{16}-\frac{35w^8}{64}+\ldots\right)$ for w << 1 $=rN^2\left\{\left(1+\frac{1}{32w^2}+O(\frac{1}{w^4})\right)\ln 8w-1/2+\frac{1}{128w^2}+O(\frac{1}{w^4})\right\}$ for w >> 1	N: Number of turns r: Radius l: Length $w=r/l$ $m=4w^2$ E,K: Elliptic integrals
Coaxial cable, high frequency	$\frac{l}{2\pi}\ln\frac{a_1}{a}$	a_1: Outer radius a: Inner radius l: Length
Circular loop	$r\cdot\left(\ln\frac{8r}{a}-2+Y\right)$	r: Loop radius a: Wire radius
Rectangle	$\frac{1}{\pi}\left(b\ln\frac{2b}{a}+d\ln\frac{2d}{a}-(b+d)(2-Y)+2\sqrt{b^2+d^2}-b\cdot\operatorname{arsinh}\frac{b}{d}-d\cdot\operatorname{arsinh}\frac{d}{b}\right)$	b, d: Border length d >> a, b >> a a: Wire radius
Pair of parallel wires	$\frac{l}{\pi}\left(\ln\frac{d}{a}+Y\right)$	a: Wire radius d: Distance, d ≥ 2a l: Length of pair
Pair of parallel wires, high frequency	$\frac{l}{2\pi}\operatorname{arcosh}\left(\frac{d^2}{2a^2}-1\right)=\frac{l}{\pi}\operatorname{arcosh}\left(\frac{d}{2a}\right)=\frac{l}{\pi}\ln\left(\frac{d}{2a}+\sqrt{\frac{d^2}{4a^2}-1}\right)$	a: Wire radius d: Distance, d ≥ 2a l: Length of pair
Wire parallel to perfectly conducting wall	$\frac{l}{2\pi}\left(\ln\frac{2d}{a}+Y\right)$	a: Wire radius d: Distance, d ≥ a l: Length
Wire parallel to conducting wall, high frequency	$\frac{l}{4\pi}\operatorname{arcosh}\left(\frac{2d^2}{a^2}-1\right)=\frac{l}{2\pi}\operatorname{arcosh}\left(\frac{d}{a}\right)=\frac{l}{2\pi}\ln\left(\frac{d}{a}+\sqrt{\frac{d^2}{a^2}-1}\right)$	a: Wire radius d: Distance, d ≥ a l: Length

Table 1. Inductance of simple electrical constructions in air.

From the above formulas we see that inductance of a structure large depends on the physical attributes like length, diameter, distances, etc. In order to vary inductance in time, the technique would primarily depend on the alteration in these physical dimensions, which imply mechanical movements. Just like most mechanical systems, such a construction would suffer from limited frequency response, restricting the operation are very low frequencies, while

optical range remains a distant dream. Similar argument also holds true for capacitors and this can be verified from the following table (1) [26].

Capacitance of simple systems

Type	Capacitance	Comment
Parallel-plate capacitor	$\varepsilon A/d$	A: Area d: Distance
Coaxial cable	$\frac{2\pi\varepsilon l}{\ln(a_2/a_1)}$	a_1: Inner radius a_2: Outer radius l: Length
Pair of parallel wires [17]	$\frac{2\pi\varepsilon l}{\operatorname{arcosh}\left(\frac{d^2}{2a^2}-1\right)} = \frac{\pi\varepsilon l}{\operatorname{arcosh}\left(\frac{d}{2a}\right)} = \frac{\pi\varepsilon l}{\ln\left(\frac{d}{2a}+\sqrt{\frac{d^2}{4a^2}-1}\right)}$	a: Wire radius d: Distance, d > 2a l: Length of pair
Wire parallel to wall [18]	$\frac{4\pi\varepsilon l}{\operatorname{arcosh}\left(\frac{2d^2}{a^2}-1\right)} = \frac{2\pi\varepsilon l}{\operatorname{arcosh}\left(\frac{d}{a}\right)} = \frac{2\pi\varepsilon l}{\ln\left(\frac{d}{a}+\sqrt{\frac{d^2}{a^2}-1}\right)}$	a: Wire radius d: Distance, d > a l: Wire length
Concentric spheres	$\frac{4\pi\varepsilon a_1 a_2}{a_2-a_1}$	a_1: Inner radius a_2: Outer radius
Two spheres, equal radius [19][20]	$2\pi\varepsilon a\sum_{n=1}^{\infty}\frac{\sinh\left(\ln\left(D+\sqrt{D^2-1}\right)\right)}{\sinh\left(n\ln\left(D+\sqrt{D^2-1}\right)\right)}$ $= 2\pi\varepsilon a\left\{1+\frac{1}{2D}+\frac{1}{4D^2}+\frac{1}{8D^3}+\frac{1}{8D^4}+\frac{3}{32D^5}+O\left(\frac{1}{D^6}\right)\right\}$ $= 2\pi\varepsilon a\left\{\ln 2+\gamma-\frac{1}{2}\ln\left(\frac{d}{a}-2\right)+O\left(\frac{d}{a}-2\right)\right\}$	a: Radius d: Distance, d > 2a D = d/2a γ: Euler's constant
Sphere in front of wall [21]	$4\pi\varepsilon a\sum_{n=1}^{\infty}\frac{\sinh\left(\ln\left(D+\sqrt{D^2-1}\right)\right)}{\sinh\left(n\ln\left(D+\sqrt{D^2-1}\right)\right)}$	a: Radius d: Distance, d > a D = d/a
Sphere	$4\pi\varepsilon a$	a: Radius
Circular disc	$8\varepsilon a$	a: Radius
Thin straight wire, finite length [22][23][24]	$\frac{2\pi\varepsilon l}{\Lambda}\left\{1+\frac{1}{\Lambda}(1-\ln 2)+\frac{1}{\Lambda^2}\left[1+(1-\ln 2)^2-\frac{\pi^2}{12}\right]+O\left(\frac{1}{\Lambda^3}\right)\right\}$	a: Wire radius l: Length Λ: ln(l/a)

Table 2. Capacitance of simple electrical systems

7.1. Selection of the Transformer

Given these concerns, it is really difficult to achieve a true inductance which can be varied in time, and show good response at high frequencies. There are certain techniques for implementing variable inductors, one of which suggest the transformer's secondary to be used as an inductor. The inductance of secondary is varied by changing the permeability of the core

using primary current variations, and B-H relation for the core [21][22]. A general L-I relation for such a construction is shown below with some arbitrary operating points.

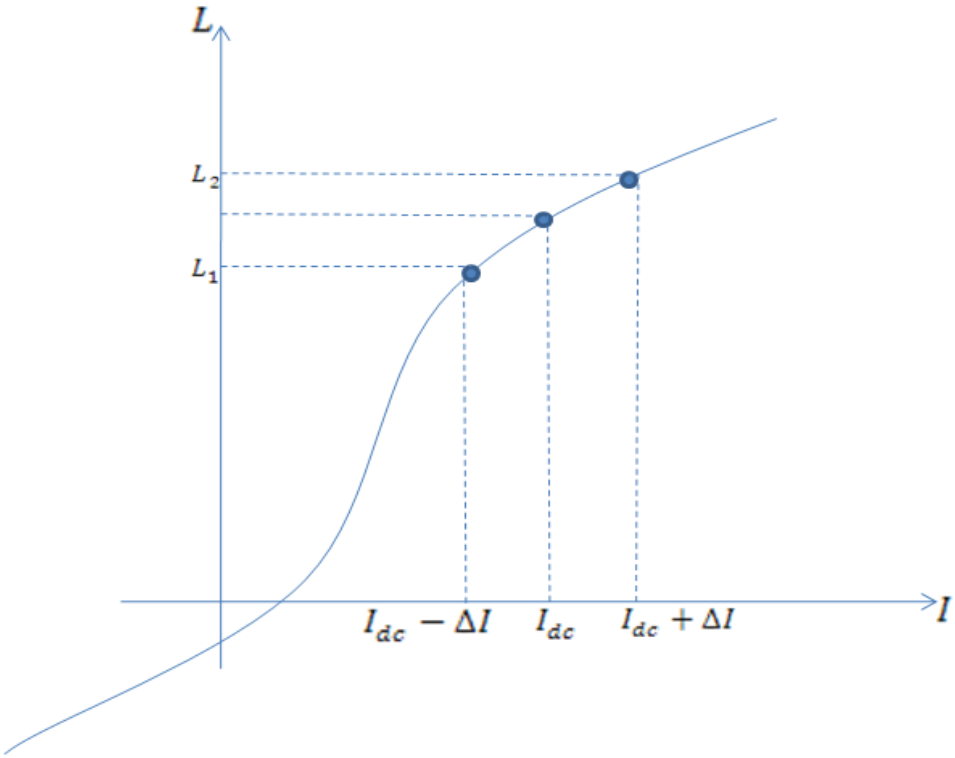

Figure 45. A typical LI curve

This is a typical curve for BH or LI relation, but the actual curve would vary from transformer to transformer. For our application it was decided, after discussion with Prof. McNeill, that the transformer would need typically low leakage inductance and a stable primary inductance with temperature since constant dc current losses in the form of heat shouldn't deviate the operating point at stray. These considerations help us go with ADSL transformers with more than or equal to three winding on iron core, and NOT air core. The data sheet of these transformers is found on the coil craft website, and is shown below in table (3) [27]

SPECIFICATIONS

Part number	Style	Chip set	Inductance (mH)	Leakage inductance max (µH)	DCR max (Ohms)	
					Chip side	Line side
AS8952-A	SMT	Titanium Fourte G7266	0.474 ±10%[1]	5	0.48 (1-4, 2-5)	0.88 (10-7, 9-6)
AS8954-A	SMT	Titanium Fourte G7266RT	0.440 ±5%[1]	5	0.36 (1-4, 2-5)	0.94 (10-7, 9-6)
AS8330-A	SMT	Titanium G7000	0.430 ±10%[2]	10	0.29 (10-7, 9-6)	0.32 (1-4, 2-5)
AS8424-A	SMT	Globespan EL-1501	0.407 ±5%[2]	10	0.363 (10-7, 9-6)	0.429 (1-4, 2-5)
AS8343-A	Leaded	GlobeSpan	0.940 ±10%[3]	10	1.0 (1-3, 2-4)	0.750 (9-7, 10-8)
AS8344-A	Leaded	GlobeSpan	0.410 ±10%[3]	10	0.340 (1-3, 2-4)	0.340 (9-7, 10-8)
AS8345-A	Leaded	GlobeSpan	0.940 ±10%[3]	15	1.0 (1-3, 2-4)	1.0 (9-7, 10-8)
AS8346-A	Leaded	GlobeSpan	0.410 ±10%[3]	10	0.340 (1-3, 2-4)	0.80 (9-7, 10-8)

Part number	Dielectric strength (V)	Turns ratio line:chip	Capacitance max (pF)	Longitudinal balance min (dB)	THD max (dB)	Designed to meet
AS8952-A	1875	1.41:1	40	55 (20 kHz – 1.1 MHz)	-90 @ 20 kHz	UL 1950
AS8954-A	1875	2:1	40	55 (20 kHz – 1.1 MHz)	-90 @ 20 kHz	UL 1950
AS8330-A	1875	1:1	40	40 (20 kHz – 1.1 MHz)	-80 @ 20 kHz	UL 1459, 1950
AS8424-A	1875	1:1	25	55 (20 kHz – 1.1 MHz)	-85 @ 20 kHz	UL 1459, 1950
AS8343-A	1500	1:1:1.4:1.4	90	50 @ 40 kHz	-80 @ 20 kHz	
AS8344-A	1500	1:1:1:1	90	50 @ 40 kHz	-80 @ 20 kHz	
AS8345-A	3000	1:1:1.4:1.4	90	55 @ 40 kHz	-70 @ 20 kHz	UL 1950
AS8346-A	3000	1:1:1:1	90	55 @ 40 kHz	-65 @ 20 kHz	UL 1950

Table 3. Datasheet of ADSL transformers

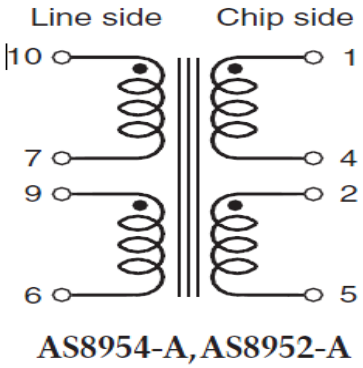

Figure 46. A constructional representation of ADSL transformer

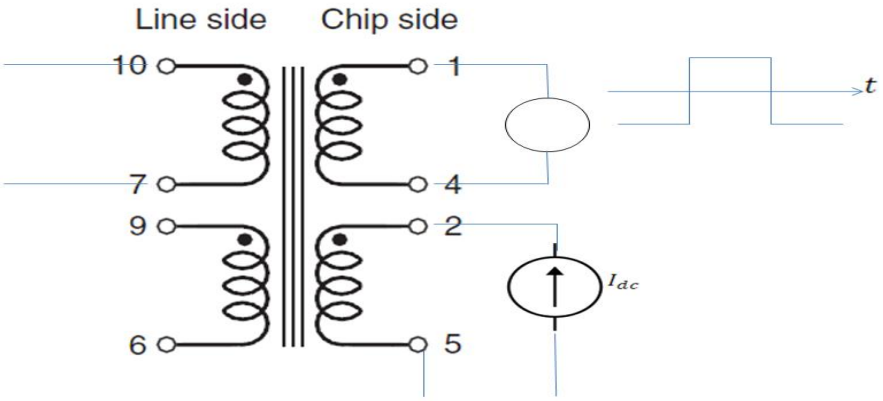

Figure 47. A generalized system for inductance switching using ADSL transformer

Figure (47), above, demonstrates the idea of how a typical ADSL transformer could be used to vary the inductance using square waveform of desired period and duty cycle. This variation on the controlling current will switch the operating point on the L-I current between two points as shown in figure (45), above. First step in engineering the material is to study the various L-I curves of these ADSL transformers, and select the curve which suits best. This means we need to select the curve and the two operating points such the wave impedances at the two operating points are exactly (or nearly to best approximation) the same, and for that we need to consider the selection of capacitors. Also note that as the testing phase, we need not be very particular about the frequency of operation. Such inductors could be used at RF range and hence we can always start here for verification of the principle at least.

7.2. Selection of the Capacitor

Varactor diodes used as voltage controlled capacitors are a good point to start with. Select the inductors with few hundreds of μH as offered by the best available ADSL transformer and then select the best match of capacitor to achieve equal impedance condition for both materials. This needs a study of CV characteristic of various diodes. We can start using 830 series of silicon 25V hyperabrupt varactor diodes. These diodes have very close tolerance of CV characteristics, absolutely essential for our plan of approach. The datasheet for these are available from the Digikey website, and the components could be directly ordered from them [28]. The datasheet for this series is shown below in table (4).

Part	Capacitance (pF) V_R=2V, f=1MHz			Min Q V_R = 3V f = 50MHz	Capacitance ratio C_2 / C_{20} @ f = 1MHz	
	Min.	Nom.	Max.		Min.	Max.
829A	7.38	8.2	9.02	250	4.3	5.8
829B	7.79	8.2	8.61	250	4.3	5.8
830A	9.0	10.0	11.0	300	4.5	6.0
830B	9.5	10.0	10.5	300	4.5	6.0
831A	13.5	15.0	16.5	300	4.5	6.0
831B	14.25	15.0	15.75	300	4.5	6.0
832A	19.8	22.0	24.2	200	5.0	6.5
832B	20.9	22.0	23.1	200	5.0	6.5
833A	29.7	33.0	36.3	200	5.0	6.5
833B	31.35	33.0	34.65	200	5.0	6.5
834A	42.3	47.0	51.7	200	5.0	6.5
834B	44.65	47.0	49.35	200	5.0	6.5
835A	61.2	68.0	74.8	100	5.0	6.5
835B	64.6	68.0	71.4	100	5.0	6.5
836A	90.0	100.0	110.0	100	5.0	6.5
836B	95.0	100.0	105.0	100	5.0	6.5

Table 4. Datasheet for 830 series, Silicon 25V hyperabrupt varactor diodes.

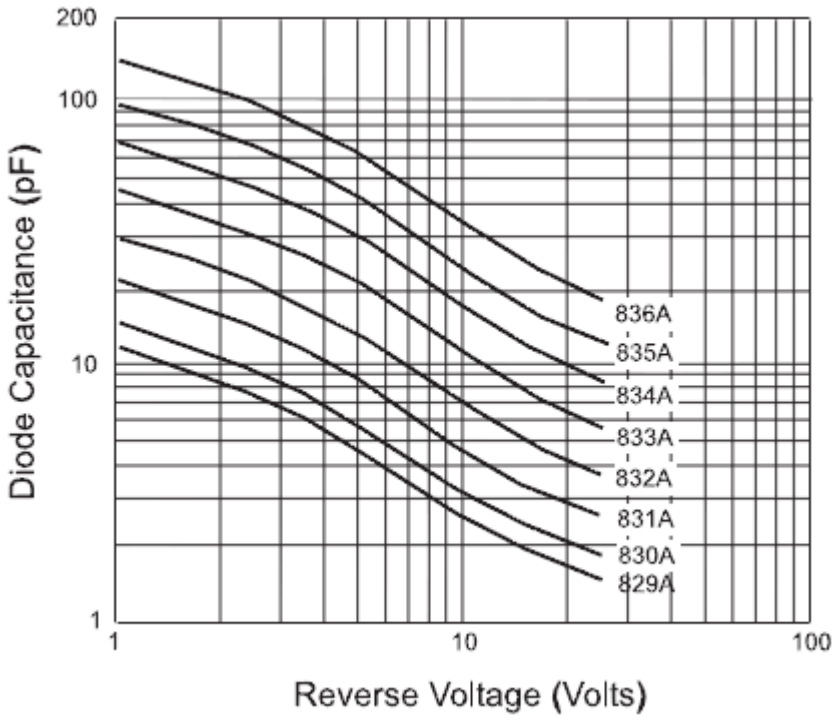

Figure 48. CV characteristics of 830 series, Silicon 25V hyperabrupt varactor diodes

The selection of the capacitor and the operating region should be based on two considerations. Firstly, the wave impedance for both materials should be the same, hence the ratio of L to C. And secondly, the characteristics of both should be very closely matched, since during transition phase, we must minimize the possible mismatch in the wave impedances and hence reflects of waves at the boundaries of checkerboard.

Once we work our way through this process of component selection, we could possibly model the system again in Spice, but this time with the new approach and exact models of these selected components. This would give us a picture much closer to reality, since it would reflect many practical constraints involved while working with real world components. Hopefully, we find some success and step ahead to create a PCB design for this system, which is the ultimate goal of manufacturing a dynamic material, and checkerboard structure working as predicted.

References

[1]	Wikipedia. "Metamaterials." http://en.wikipedia.org/wiki/Metamaterial, 2009
[2]	K. A. Lurie and S. L. Weekes, "Some advances in the theory of Dynamic materials", Proc. International Conference "Physics and Control", St. Petersburg, Russia, 2003.
[3]	K. A. Lurie, "The problem of effective properties of a mixture of two isotropic dielectrics distributed in space-time and the conservation law for wave impedance in 1D wave propagation," Proc. Roy. Soc. London Ser. A 454 (1998) 1767-1779.
[4]	H. J. Eichler, "Introduction to the special issue on dynamic gratings and four-wave mixing", IEEE J. Quantum Electronics 22 (1986) 1194-1995.
[5]	K. A. Lurie, "Effective properties of smart elastic laminates and the screening phenomenon", Internat. J. Solids Structures 34 (1997) 1633-1643.
[6]	S. L. Weekes, "Numerical computation of wave propagation in dynamic materials", Appl. Numer. Math. 37 (2001) 417-440.
[7]	K. A. Lurie, "Low frequency longitudinal vibrations on an elastic bar made of a dynamic material and excited at one end", J. Math. Anal. Appl. 251 (2000) 364-375.
[8]	K. A. Lurie, "Bounds for the electromagnetic material properties of a spatio-temporal dielectric polycrystal with respect to 1D wave propagation", Proc. Roy. Soc. London Ser. A 456 (2000) 1547-1557.
[9]	K. A. Lurie, S. L. Weekes, "Effective and averaged energy densities in 1D wave propagation through spatio-temporal dielectric laminates with negative effective values of ϵ and μ, in R, Agarwal, Nonlinear Analysis and Application, Kluwer Academic, 2004, pp. 767-789.
[10]	S. L. Weekes, "A stable scheme for the numerical computation of long wave propagation in temporal laminates", J. Comput. Phys. 176 (2002) 345-362.
[11]	S. L. Weekes, "A dispersive effective equation for wave propagation through dynamic laminates, Wave Motion 38 (2003) 25-41.
[12]	http://powerelectronics.com/mag/power_spice_analog_behavioral/ Christophe Basso, "Spice analog behavioral modeling of Analog passives" – Resistor, Power Electronics Technology, March 2005.
[13]	http://powerelectronics.com/mag/power_spice_analog_behavioral/ Christophe Basso, "Spice analog behavioral modeling of Analog passives" – Capacitor, Power Electronics Technology, April 2005.

[14]	http://powerelectronics.com/mag/power_spice_analog_behavioral/ Christophe Basso, "Spice analog behavioral modeling of Analog passives" – Inductor, Power Electronics Technology, May 2005.
[15]	D. J. Graffiths, "Introduction to Electrodynamics", 3rd Edition, Pg 375.
[16]	K. A. Lurie, S.L. Weekes, "Wave propagation and energy exchange in a spatio-temporal material composite with rectangular microstructure", J. Math. Anal. Appl. 314 (2006) 286-310.
[17]	F. R. Morgenthaler, "Velocity Modulation of Electromagnetic Waves", IEEE, IRE Transactions on Microwave theory and Techniques, Vol. 6, Issue 2, April 1958, Pg 167-172.
[18]	K. A. Lurie, D. Onofrei, S. L. Weekes, "Mathematical analysis of the wave propagation through a rectangular material structure in space-time", J. Math. Anal. Appl. 355 (2009) 180-194.
[19]	Wikipedia. "RC Circuit". http://en.wikipedia.org/wiki/RC_circuit
[20]	Wikipedia. "RL Circuit". http://en.wikipedia.org/wiki/RL_circuit
[21]	United States Patent No. 7242275, Issued on July 10th, 2007
[22]	Medini, D., and Ben-Yaakov, S., "A Current-Controlled Variable-Inductor for High Frequency Resonant Power Circuits", *IEEE,* 219:225, (1994).
[23]	LTSpice group on yahoo groups- http://groups.yahoo.com/group/LTspice
[24]	Matlab Central, file exchange – "Fast import of compressed Binary .RAW files Created with LTspice Circuit Simulator". http://www.mathworks.com/matlabcentral/fileexchange/23394-fast-import-of-compressed-binary-raw-files-created-with-ltspice-circuit-simulator
[25]	Wikipedia. "Inductance". http://en.wikipedia.org/wiki/Inductance, 2009.
[26]	Wikipedia. "Capacitance". http://en.wikipedia.org/wiki/Capacitance, 2009.
[27]	Coilcraft website, xDSL transformer types, datasheets http://www.coilcraft.com/xdsltran.cfm, 2009.
[28]	Digi-Key Corporation website, 830 Series, Silicon varactor diodes datasheets http://search.digikey.com/scripts/DkSearch/dksus.dll?vendor=0&keywords=ZC830, 2009.

Appendix A – Spice Netlists for variable passives

Variable Inductor

```
.subckt variable 1 2 CTRL
BC 1 2 I=V(INT)/V(CTRL)
BINT 0 INT I=V(1,2)
CINT INT 0 1
R1 CTRL 0 10
.ends variable
```

Variable Capacitor

```
.subckt  variable  1  2  CTRL
BC  4  2  V=V(INT)/V(CTRL)
BINT  0  INT  I=I(VC)
CINT  INT  0  1
R2  CTRL  0  10
VC  1  4
.ends  variable
```

Appendix B – Spice Netlist for an LC unit of Transmission line

```
.subckt variablelc2 1 2 CTRL
XX1 1 2 N002 variablel
XX2 2 0 N001 variablec
R1 CTRL 0 1K
B1 N002 0 V=(VL1+VL2)/2 + ((VL2-VL1)/2)*cos(pi*V(CTRL)/(Vk2-Vk1))
B2 N001 0 V=(VC1+VC2)/2 + ((VC2-VC1)/2)*cos(pi*V(CTRL)/(Vk2-Vk1))
.param VL1 480u
.param VL2 400u
.param VC1 0.48p
.param VC2 0.4p
.param Vk1 0
.param Vk2 5
.ends variablelc2
```

Appendix C – LTspice2Matlab code

The Matlab code LTspice2Matlab takes care of extracting the Spice data in binary form from .RAW file to Matlab. This file can be downloaded directly from the Mathwork website.

Link –

http://www.mathworks.in/matlabcentral/fileexchange/23394

Appendix D – Time plots and Spice codes

The time plots obtained from Spice and the codes generating them are uploaded to the esnip folder for later referencing, along with the other Spice codes. For the access to these files contact –

Prof. K. A. Lurie @ klurie@WPI.EDU

Prof. R. Ludwig @ ludwig@wpi.edu

Prof. S. L. Weekes @ sweekes@WPI.EDU

G. B. Samant @ gaja.s@wpi.edu or chetnya@gmail.com